A Brief History of OLEDs—Emitter Development and Industry Milestones

Gloria Hong, Xuemin Gan, Céline Leonhardt, Zhen Zhang, Jasmin Seibert, Jasmin M. Busch, and Stefan Bräse*

Organic light-emitting diodes (OLEDs) have come a long way ever since their first introduction in 1987 at Eastman Kodak. Today, OLEDs are especially valued in the display and lighting industry for their promising features. As one of the research fields that equally inspires and drives development in academia and industry, OLED device technology has continuously evolved over more than 30 years. OLED devices have come forward based on three generations of emitter materials relying on fluorescence (first generation), phosphorescence (second generation), and thermally activated delayed fluorescence (third generation). Furthermore, research in academia and industry toward the fourth generation of OLEDs is in progress. Excerpts from the history of green, orange-red, and blue OLED emitter development on the side of academia and milestones achieved by key players in the industry are included in this report.

1. Introduction

Organic light-emitting diodes (OLEDs) are (colored) light sources, used in displays of smartphones and TV screens as well as in panels for lighting applications. Over the past 25 years, the research and development of OLEDs became a rapidly expanding field in academia and industry. OLEDs offer a new efficient and sustainable method for lighting and display technologies and are on the rise to supersede the previous technologies on the market. Especially in the display industry, OLEDs have moved into focus in recent years as OLED displays offer some features that grant them superior properties over well-established technologies like liquid crystal displays (LCDs).

G. Hong, X. Gan, C. Leonhardt, Dr. Z. Zhang, J. Seibert, Dr. J. M. Busch, Prof. S. Bräse
Karlsruhe Institute of Technology (KIT)
Institute of Organic Chemistry (IOC)
Fritz-Haber-Weg 6, Karlsruhe 76131, Germany
E-mail: braese@kit.edu
Prof. S. Bräse
Karlsruhe Institute of Technology (KIT)
Institute of Biological and Chemical Systems–Functional Molecular Systems (IBCS-FMS)
Hermann-von-Helmholtz-Platz 1, Eggenstein-Leopoldshafen 76344 Germany

The ORCID identification number(s) for the author(s) of this article can be found under https://doi.org/10.1002/adma.202005630.

For example, OLED devices do not require a backlight system in comparison to LCDs.[1] This is not only energy-efficient as an inactive OLED element does not produce light or consume power, but also allows for a "true black" and thinner and lighter displays.[2] Moreover, OLED displays show improvements in resolution, wider viewing angles, high contrast colors, faster response time, and the possibility to realize transparent displays. A major winning argument is also the realization of flexible OLED displays that can be bent and rolled up like a poster, which opens a new dimension to the design possibilities of displays.[3] However, the technology of OLEDs still faces key challenges with its materials systems but also the OLED device architecture. A further innovation is required to increase the efficiency, lifetime, and light output of OLED devices. In addition, the reduction of the driving voltage is crucial to improve power conversion efficiency. One of the biggest issues is the short lifetime of blue OLEDs compared to red and green OLED devices. The degradation of the blue emitters and the matrix must be minimized in order to increase the device lifetime.[4] Besides the need for further research on the side of the OLED materials, the device architecture of flexible OLEDs remains an open challenge as these devices experience problems related to the thermal and chemical instability of the flexible substrates.[5]

OLEDs are typically thin multilayer devices that consist of layers of organic semiconductors (see **Figure 1**).[6] As the processes behind the light-generation in OLEDs have been previously described in further detail,[7] we only provide a short, simplified mechanism. The charge carriers, that is, electrons and holes, are obtained at the cathode and anode, respectively, by applying an external voltage. Subsequently, the charge carriers are injected into the electron and hole injection layers. Next, the electrons and holes migrate through the electron and hole transport layers into the emissive layer (EML), where the recombination of the charge carriers and the formation of excitons takes place. The electroluminescence (EL) occurs as these excitons relax radiatively from the excited state to the ground state. The rational design of the emissive layer that holds the host/dopant (emitter) system is the most critical factor in achieving high efficiency in OLED devices.[8]

This report is not intended to be an all-comprehensive summary of the ≈14 000 journal publications, 13 000 patents, over 1 000 reviews, and several books that have been released over the past decades (SciFinder-n search using "Organic Light-Emitting Diode" as search keyword on October 6th, 2020), but aims for

Figure 1. Schematic depiction of a stacked device structure of an organic light-emitting diode (OLED).

giving a brief overview of the historic development of OLEDs in industry and the OLED emitters in academia by focusing on the following three topics: i) a curated historic perspective on the emitter development on the side of academia, which includes metal-based and purely organic emitters built into green, orange-red and blue OLED devices, ii) selected information on the OLED development over the past three decades on the side of the industry, and iii) a perspective on the next up-coming "fourth generation" of light-emitting materials for OLEDs.

The academic OLED emitter development in this report is structured according to various "generations" of OLEDs which are based on the type of emission mechanism that is used to emit light. Hereby, the term "generation" is only in close approximation to the chronological order of the development. The first generation of OLEDs is using fluorescent emitters, while the second generation is based on phosphorescence and the third generation relies on thermally activated delayed fluorescence (TADF) as the light-emitting pathway. After the three well-established OLED generations, the "fourth generation" of OLED emitters will be introduced. The first three generations are subdivided into green, orange-red, and blue emitters as green OLED emitters were introduced before red, and red before blue. These three red, green, and blue colors are crucial for the color saturation of the

OLED devices. As established in earlier reviews, we will continue defining the color of the OLED by the EL wavelength as this seems to be a parameter reported for most devices.[3,9] However, for blue OLEDs, the Commission International de l'Éclairage (CIE) coordinates are as important as the wavelength for display applications and have therefore been included in the respective subchapters. The required CIE coordinates for blue OLEDs are (x,y) (0.15, 0.06) as defined by High-Definition-television ITU-RBT.709.[10] In the case that an emitting material was reported with a color range in different devices or a series of an emitter and its derivatives with various emission colors was introduced, we included the emitter and the corresponding properties of the device with the highest external quantum efficiency (EQE) value.

The development of the device structure, host materials, and other components of OLEDs will not be discussed in this work. Moreover, emitters that are exclusively reported in patents, white OLEDs, and OLEDs with emitters based on polymers are not covered within the scope of this report, even though especially the latter present a favorable option to develop large-area, printable devices in a cost-effective and solution-processable fashion.[11]

2. OLED Development in Industry

Fundamental research for the development of today's OLED technology can be traced back to the early 1960s when eosin was found to emit delayed fluorescence[12] and the application of high voltage to anthracene crystals succeeded in EL.[13] Although numerous organic compounds with fluorescence in the visible region were known, low efficiencies and high operating voltages had to be overcome, before the great potential of OLEDs was manifested.[14] In 1987, at Eastman Kodak,[15] Tang et al. built the first OLED device operated at sufficiently low voltages which marks the breakthrough of OLED technology.[14] Since then, research and development of OLED technology have continuously evolved in academia as well as in industry (see **Figure 2**).[16]

Almost ten years after the groundbreaking work at Eastman Kodak, the first commercial OLED device was produced by Pioneer and applied in car audio systems as a passive-matrix-driven display screen.[17] Following the seminal work of Burroughes et al. in 1990, polymer-based OLEDs were
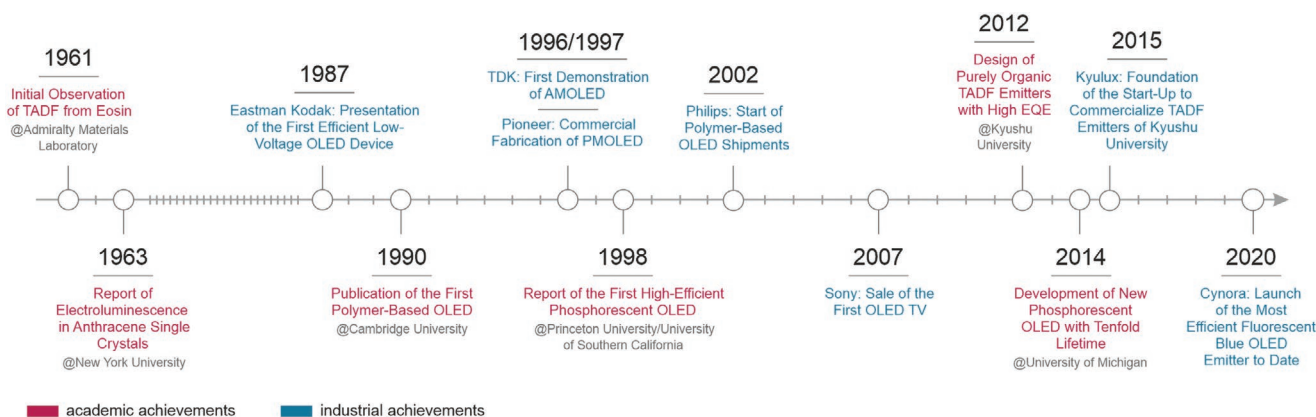
Figure 2. Overview of milestones in OLED technology; PMOLED–passive matrix OLED, AMOLED–active matrix OLED.[12,16]

**ADVANCED
SCIENCE NEWS**

www.advancedsciencenews.com

**ADVANCED
MATERIALS**

www.advmat.de

introduced to the market in 2002 by Philips.[18] Full-color active-matrix OLEDs (AMOLEDs) became available starting from 2002 when SK Display Corporation—a collaboration between Eastman Kodak Company and Sanyo Electric Company—started their mass manufacturing process.[19] The development of AMOLED was a major milestone in display technology to achieve high-resolution displays with low power consumption that were soon implemented in mobile phones like the Nokia N85 and Samsung I7710.[20] In 2007, Sony released the world's first OLED TV (XEL1) consisting of a 3 mm thin 11″ panel, and the first commercial OLED panels (HANGER, VANITY) for lighting applications were developed by Lumiotec in 2011.[21] Two years later, the flexible OLED design was commercially realized in Samsung's Galaxy Round featuring a curved 5.7″ Full HD super flexible AMOLED and LG's G-Flex with a 6″ HD curved polymer-based OLED.[22] Further R&D led to the first bendable TV panel in 2015 and the imminent release of a rollable TV was announced by LG in 2020.[23] Currently, innovative designs of foldable devices including smartphones of Royale (FlexPai), Samsung (Galaxy Fold), and Huawei (Mate X) as well as the foldable notebook of Lenovo and Intel (ThinkPad X1 Fold) have attracted much attention.[24]

To improve the overall efficiency of existing OLEDs, companies are continuously investigating new OLED materials. Earlier this year, CYNORA launched cyBlueBooster as a blue emitter exhibiting a narrow emission and superior efficiency of 15% to established emitter materials.[25] Shortly thereafter, Kyulux announced that it started to supply WiseChip with its yellow-emitting material to produce the first display based on hyperfluorescence.[26] The immense progress of OLED technology increases the anticipation of unique OLED products in the future. The overall growing interest of industry and academia in the OLED technology is also mirrored by the number of publications and patents that were filed in recent years (2000–2020) as shown in **Figure 3**.

Since organic light-emitting devices provide high contrast ratios, wide viewing angles, and can be implemented in a thin and light design, they are promising compounds for displays and lighting products.[14] The estimated volume of the OLED market size amounts to 34.3 billion USD in 2020 and is expected to increase in volume to 52 billion USD until 2023.[27] Some of the key market players in the field of OLED displays are Samsung Electronics Co. Ltd., LG Display Co. Ltd., BOE Technology Group Co. Ltd., Panasonic Corporation, Sony Corporation, JOLED Inc., Tohoku Pioneer Corporation, and Universal Display Corporation amongst many others.[28] Through the interest of both academia and industry in the OLED technology, companies, or spin-offs with close ties to or roots in academia have evolved. Prominent examples are Kyulux Inc. (Kyushu University), CYNORA GmbH (Karlsruhe Institute of Technology), C3Nano (Stanford University), Cambridge Display Technology Inc. (CDT) (University of Cambridge), Dresden Microdisplay (The Fraunhofer Institute for Photonic Microsystems), Novaled (The Fraunhofer Institute for Photonic Microsystems and TU Dresden), and Visionox Technology Inc. (Tsinghua University).[29] The trust in these companies and OLED technology has also been expressed through acquisitions and investments. Two examples of acquisitions are CDT which was acquired by the Sumitomo Chemical Group for ≈285 million USD in 2007 and Novaled which was then acquired by CHIEL Industries Inc. (now part of Samsung SDI) for 260 million Euro in 2013.[30] On the side of investments, Kyulux successfully closed its Series B funding round in 2019 where it secured ≈31.8 million USD, while CYNORA announced that it had procured 25 million USD in its Series C funding round around the same time.[31] Furthermore, a patent analysis report from Choi and co-workers from 2019 surveyed several thousand patents on TADF materials and identified some of the leading players in the field of OLED devices from both academia and industry.[32] Some of the major conferences where both sides meet are the SID Display Week, China International OLEDs Summit, International Conference on Display Technology, large-area, organic & printed electronics convention, OLED Korea Conference, OLEDs World Summit, Electronics Display Conference, and SPIE Photonics West.

In summary, OLEDs are crucial to the efforts of the development and production of superior, innovative displays. The extensive amount of R&D as represented by the number of patents, as well as investments into this field, not only demonstrates the keen interest and trust in this technology, but also the anticipated customer demand.

3. Emitters for Application in OLEDs

For OLED devices, the generated singlet excitons and triplet excitons are in a 25% to 75% ratio. To obtain satisfying device performances with high EQEs, the development and design of light-emitting materials for OLEDs emitting materials, which have the potential to fully harvest the singlet excitons and triplet excitons, are of utmost importance. Three generations of emitters have been elaborately studied and developed to realize this goal and the next generation of emitters is currently being developed in parallel.

3.1. First Generation Emitters

The first-generation OLEDs are known as fluorescent OLEDs, which typically employ organic dyes. Since the intersystem

Figure 3. Comparison of the number of publications and patents found on SciFinder.cas.org with the buzz word and concept "OLED" indicating the interest in the field of OLEDs between 2000 and 2020 as of October 09th, 2020.

crossing (ISC) transition between states of different electronic spin multiplicity is non-radiative, only the transition of singlet excitons to the singlet ground state ($S_1 \rightarrow S_0$) is theoretically allowed for fluorescence. Therefore, only about 25% of the singlet excitons can be harvested for luminescence. The upper limit of the EQE of OLEDs using conventional fluorescent emitters is 5% without additional optical outcoupling.

3.1.1. First Generation: Green Emitters

The first well-designed OLED device was reported by Tang and VanSlyke in 1987.[33] The fluorescent emitter 8-hydroxyquinoline aluminum (Alq$_3$) shown in **Figure 4** was used as an emitter in a vacuum-deposited device. The device performed with an EQE of 1% with a brightness of over 1 000 cd m^{-2} and an EL wavelength in the green spectral region at 550 nm at a driving voltage of less than 10 V. Based on these results, the field of OLEDs was founded and has continuously received attention ever since.

3.1.2. First Generation: Orange-Red Emitters

The first red-dopant-based red OLED was introduced in 1989 by Chen and co-workers.[34] They reported two orange-red OLED devices based on 4-(dicyanomethylene)-2-methyl-6-[4(dimethylaminostyryl)-4H-pyran] (DCM) emitters DCM1 and DCM2 as shown in Figure 4. They showed EL in the wavelength ranges of λ_{EL} (DCM1) = 570–620 nm and λ_{EL} (DCM2) = 610–650 nm, dependent on the doping

concentration, and EQEs of 2.3%. However, in general, red fluorescent materials were mostly limited to the dopant usage as emitters in the fabrication of red OLEDs, instead of being used in non-doped devices, because of concentration-dependent aggregation-caused quenching. Emitters with a wavelength of $\lambda_{max} > 610$ nm were typically based on polar structures or non-polar but π-conjugated molecule designs.[35] These design characteristics inherently led to aggregation in solid state due to attractive dipole-dipole interactions or effective intermolecular π-stacking. Consequently, concentration quenching resulted in weakly emissive or even non-emissive fluorophores in solid-state. Moreover, it soon became clear that dopant-based red OLEDs needed further improvement as efficient and bright dopants were not red enough, and red enough dopants were not efficient and bright.[35] Thus, the assist dopant approach was developed by Usuki and co-workers in 1999 that solved the problem of concentration quenching of red dopants by introducing an emitting assist dopant such as rubrene that filled the gap of energy transfer between the host and the red dopant.[36] Besides the doped red OLEDs, the first host-emitting non-doped red OLED was introduced by Hasegawa and co-workers in 2000.[37]

3.1.3. First Generation: Blue Emitters

Blue fluorescent emitter materials are often based on anthracene derivatives. These show a wide bandgap, rigid chemical structure, good thermal stability as well as excellent charge-transporting properties.[38] By introducing bulky substituents to
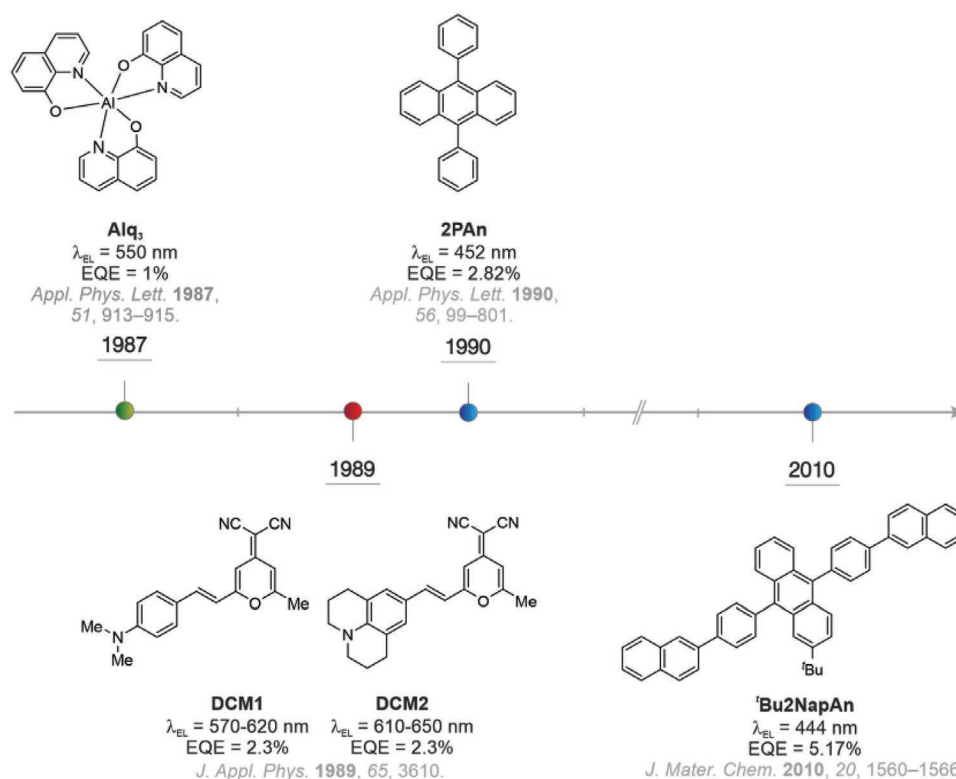
Figure 4. A selection of first-generation OLED emitters based on fluorescent molecules.

the 9- or 10-position, the emission color is shifted from blue to deep blue. A non-doped device based on the fluorescent emitter **2PAn** shown in Figure 4 showed an EQE of 2.82%, an emission wavelength at 452 nm, and CIE coordinates of (0.71, 0.21).[39] The CIE coordinates are not ideal which is caused by the aggregation of the molecules in the thin film which quenches the fluorescence and red-shifts the emission spectrum. In comparison, emitter ^{t}Bu2NapAn (see Figure 4) shows an excellent deep blue emission with CIE coordinates (0.149, 0.086) and a better efficiency with an EQE of 5.17% at a wavelength of 444 nm because the *tert*-butyl group suppresses aggregation.[40]

3.2. Second Generation Emitters

To get access to the remaining 75% of excitons in triplet states, phosphorescent heavy-metal complexes have been investigated and developed as emitters for the second generation of OLEDs.[41] Through an enhanced spin-orbit coupling induced by heavy-metal atoms such as iridium or platinum, the resulting complexes can accelerate the radiative deactivation through phosphorescence from the lowest-lying triplet state T_1 to the ground state S_0 and facilitate ISC from the lowest-lying singlet state S_1 to T_1. This triplet-using strategy and relaxation pathway allow phosphorescent heavy-metal-based emitters to reach internal quantum efficiency (IQE) up to 100%, which is crucial to obtain OLED devices with high EQEs.

3.2.1. Second Generation: Green Emitters

Since the pioneering work of Watts and co-workers in 1991 for the preparation of *fac*-tris(2phenylpyridine)iridium *fac*-Ir(ppy)$_3$ (see **Figure 5**), this emitter has been widely applied as a green-emitting dopant in OLED devices due to its excellent stability and electroluminescent performance.[42]

Forrest and co-workers firstly introduced it in 1999 in a green phosphorescent OLED (PhOLED) with an emission wavelength of 510 nm and a peak EQE of 8%.[43] In their subsequent research, the photochemical isomerization of facial (*fac*-) and meridonal (*mer*-) tri-cyclometallated Ir(III) complexes was investigated regarding their electrochemical and photophysical behavior.[44] Compared with *mer*-Ir(C^N)$_3$ complexes, the thermodynamically favored facial isomers have identical bond lengths in principle. This most likely suppresses the quenching pathway, leading to higher quantum efficiencies. Many
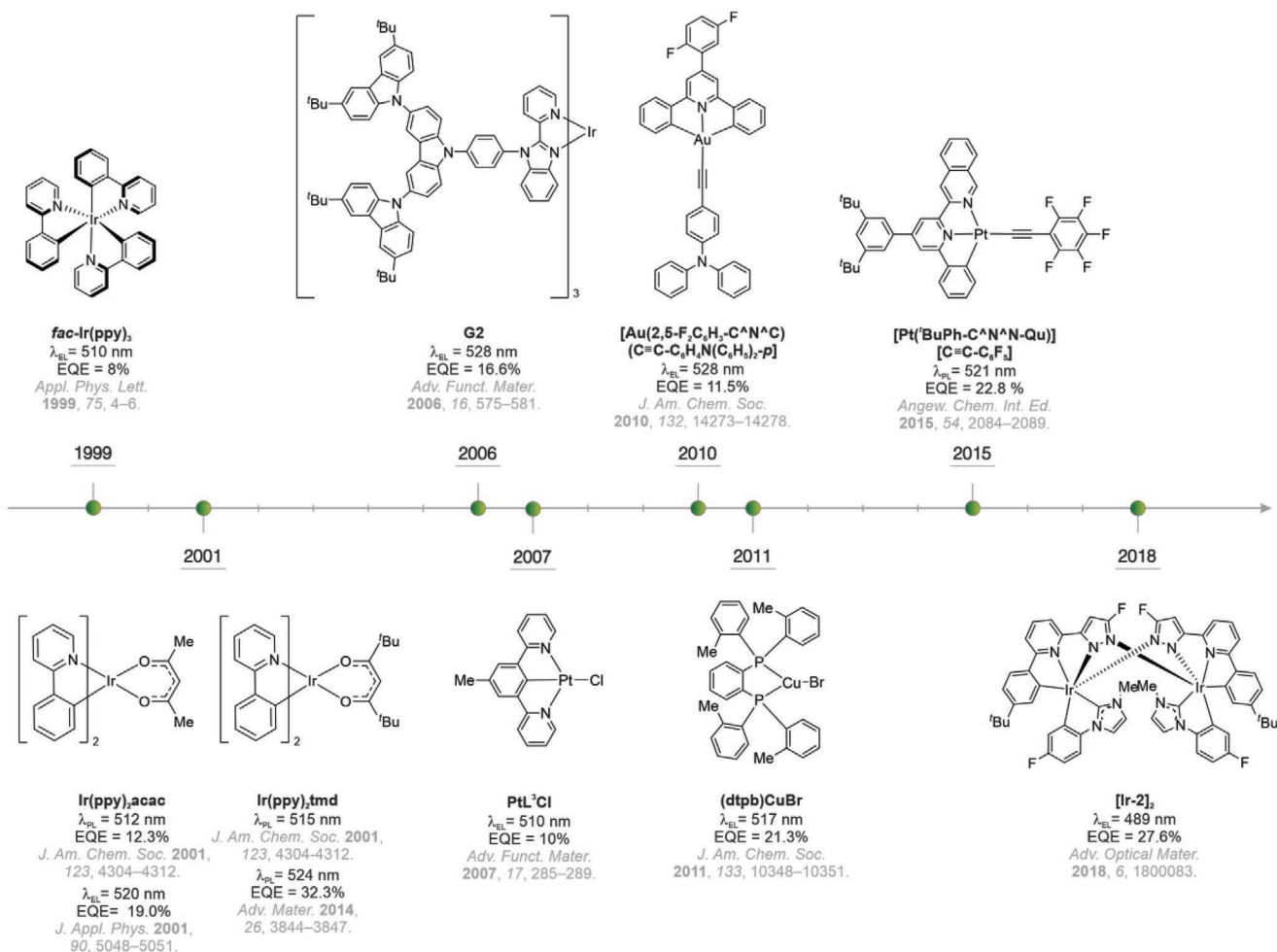
Figure 5. The second generation of green OLED emitters is based on phosphorescent molecules.

**ADVANCED
SCIENCE NEWS**

www.advancedsciencenews.com

**ADVANCED
MATERIALS**

www.advmat.de

functional ancillary ligands with different ligand field strengths have also been employed for bis- or tris-cyclometalated Ir(III) complexes for color-switchable OLEDs.[45] In 2001, Thomson and co-workers demonstrated vapor-deposited PhOLEDs based on heteroleptic (C^N)$_2$Ir(acac) complexes (acac = acetylacetonate, C^N = cyclometalated bidentate ligand) as the emitting dopants.[46] These (C^N)$_2$Ir(acac)-doped PhOLEDs show a broad range of emission color from green to red. Among them, the highest EQE of 12.3% with a λ_{EL} = 525 nm was observed in the green OLED device employing Ir(ppy)$_2$acac, shown in Figure 5, as the doped emitter. Another complementary strategy for color-tuning of Ir(III)-based triplet emitters is the introduction of various functional groups X (X = SiPh$_3$, NPh$_2$, B(Mes)$_2$, OPh, SPh, etc.) to the phenyl ring of ppy in [Ir(ppy-X)$_2$(acac)] complexes.[47] The ppy-type cyclometalated Ir(III) complexes depicted in Figure 5 were used as emitters to construct OLEDs showing moderate EQE values of 4–16% with EL emission wavelengths in 505–609 nm.

The ancillary ligands with different ligand field strengths for bis- or tris-cyclometalated Ir(III) complexes have also been employed as photoemitters for OLEDs.[48] Wang and co-workers introduced the rigid carbazole dendron to the Ir(C^N)$_3$ complexes, giving the G2 dendrimer (see Figure 5) with a high PL quantum yield of 87% in solution.[49] When G2 is doped into a carbazole-based host, the resulting PhOLED shows a high brightness above 20 000 cd m^{-2}, a maximum EQE of 16.6%, and an EL wavelength of 528 nm.

In 2014, Kim and co-workers studied the influence of the orientation on the well-designed Ir(ppy)$_3$, Ir(ppy)$_2$acac, and Ir(ppy)$_2$tmd (ppy = 2-phenylpyridine, tmd = 2,2,6,6-tetramethylheptane-3,5-dionate) (see Figure 5).[50] It is worth noting that Ir(ppy)$_2$tmd with a high horizontal dipole ratio of 78% resulted in a high photoluminescence quantum yield (PLQY) of 96%. Employing Ir(ppy)$_2$tmd as the emitter, a bottom emission OLED with an outstanding EQE of 32.3% was realized, which is one of the most excellent green OLEDs.

Next to Ir-based emitters, Pt-based complexes that possess long-lived emissive excited states in the order of μs were investigated for the application in PhOLEDs. Early attempts to use the [Pt(C^N)(O^O)] (O^O = β-diketonate ligand) monomer and excimer as the dopants in OLEDs were conducted by Forrest and co-workers.[51] The tridentate cyclometalated Pt(II) complexes of conjugated aryl-substituted diphenylpyridines (N^N^C- or N^N^C-units) show intense triplet metal-to-ligand charge transfer (MLCT) emission and good film-forming capability and the complexes have subsequently been used in OLED applications.[45,52]

In 2007, Williams and co-workers reported the pincer Pt(II) complex [PtL^{3}Cl] as depicted in Figure 5 with an additional methyl group that displays intense green phosphorescence in solution.[53] The OLED device using PtL^{3}Cl as emitting dopant exhibited an EQE up to 10%, an emission wavelength of 510 nm, and the peak current efficiency of 30 cd A^{-1}. In 2015, Che and co-workers developed several novel pincer Pt(II) complexes bearing C-deprotonated C^N^N ligands with different extended π-conjugation.[54] The best device utilizing the phosphorescent [Pt(^{t}BuPh-C^N^N-Qu)][C≡CC$_6$F$_5$] emitter as shown in Figure 5, exhibited a green emission with CIE coordinates of (0.368, 0.598) at an EQE of 22.8%.

Recently, considerable efforts have been made to investigate a new class of d^{10} metal complexes with great optical properties for the application in PhOLEDs. Yam and co-workers realized a solution-processed PhOLEDs based on the strongly luminescent Au(III) complex [Au(2,5-F$_2$C$_6$H$_3$−C^N^C) (C≡C−C$_6$H$_4$N(C$_6$H$_5$)$_2$-p] shown in Figure 5, as early as in 2010.[55] A respectable EQE of up to 11.5%, an EL wavelength of λ_{EL} = 528 nm, and current efficiency of 37.4 cd A^{-1} were achieved. Subsequently, alkynylgold(III) complexes based on the κ^3-(C^N^C) pincer ligands (N = pyridine or pyrazine) have also been proposed as low-cost dopant candidates for promising PhOLEDs with high EQEs above 10%.[56] In 2011, Hashimoto and co-workers reported the fabrication of green OLEDs derived from three-coordinate Cu(I) complexes (dtpb) CuBr with the 1,2-bis(oditolylphosphino)benzene] (dtpb) ligand as depicted in Figure 5, leading to high efficiencies up to 21.3% for the peak EQE and 520 nm for the emission wavelength.[57]

3.2.2. Second Generation: Orange-Red Emitters

In 1998, Forrest and co-workers reported the first effective PhOLED using red-emitting 2,3,7,8,12,13,17,18-octaethyl21H, 23H-porphine platinum (II) (PtOEP) as shown in **Figure 6**, achieving a peak EQE of 4%.[58]

During the next decades, significant effort to the PhOLED field has been made to improve the device performance employing phosphorescent complexes for multicolor displays. Red phosphorescent emitters are less abundant due to the difficulty in suppressing triplet-triplet annihilation and achieving effective radiative decay of MLCT states. From a fundamental perspective, per-deuterated and per-fluorinated approaches, which have been employed by decreasing the number of high-frequency vibrations associated with C−H, O−H, and N−H stretching, are two feasible ways to suppress the quenching process and reduce the vibrational overlap.[59] The cyclometalated neutral Ir(III) complexes are widely regarded as promising candidates for efficient red PhOLEDs. The majority of the reported neutral red phosphors based on the 1-phenylisoquinoline, 2-phenylquinoline, or acetylacetonate ligand are the β-diketonate-based complexes or homoleptic complexes.[60] For the acetylacetonate-based red phosphors, Thompson and co-workers reported bis(2-(2′-benzo[4,5-a]thienyl)pyridinato-N,C$^{3'}$) iridium(acetylacetonate) Btp$_2$Ir(acac) (see Figure 6) as a red emitter for an OLED device with emission wavelengths at 616 nm and a high EQE (≈7%).[46] Another well-known red luminophore is tris[1phenylisoquinoline-C2,N]iridium(III) Ir(piq)$_3$ which is also depicted in Figure 6.[61] It was investigated by Hoshino and co-workers in 2003 and showed a k_r value approximately one order of magnitude larger than other members of the Ir(C−N)$_3$ family. The EQE of the corresponding device was reported to be 12.3% with λ_{EL} = 620 nm. Substituting aromatic ligands with electron donor groups substituents, such as methoxy and amine groups, generally red-shifts the emission due to the competing σ-withdrawing character of the ligands, which leads to a destabilization of the highest occupied molecular orbital (HOMO) level.[60]

**ADVANCED
SCIENCE NEWS**

www.advancedsciencenews.com

**ADVANCED
MATERIALS**

www.advmat.de
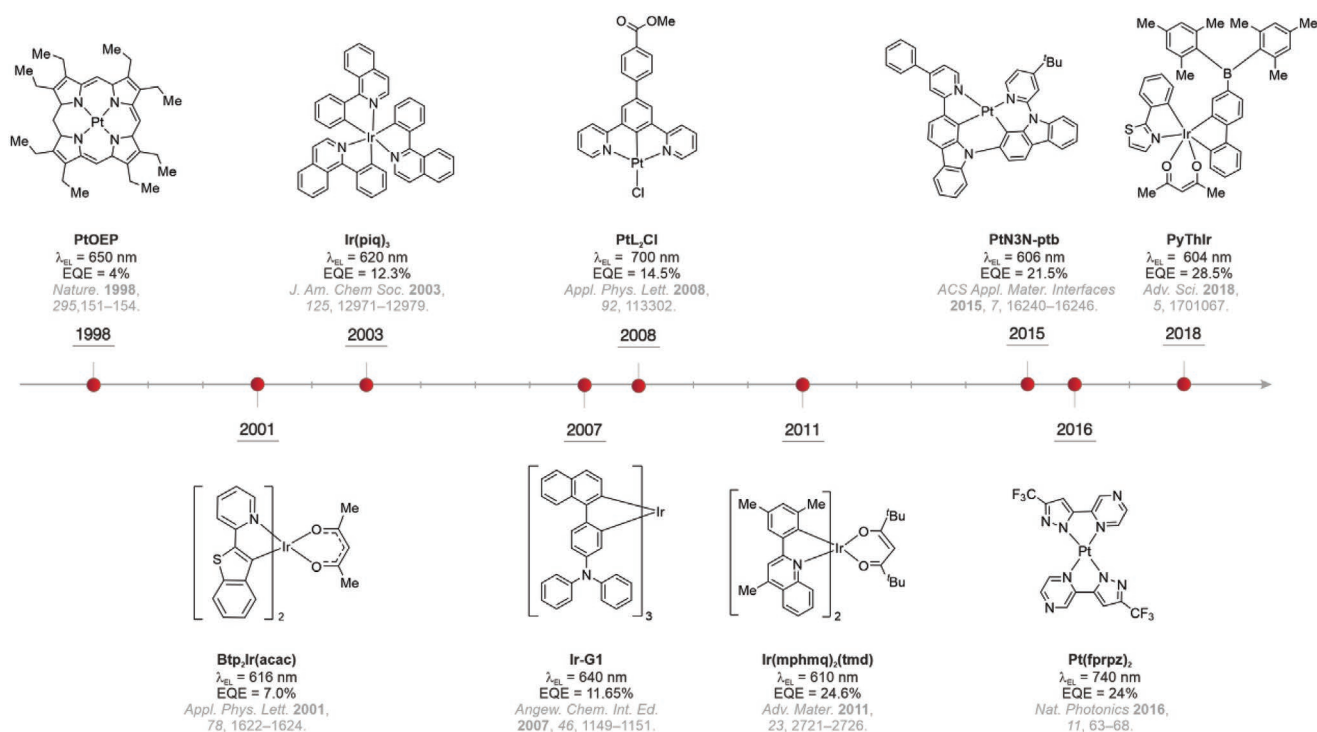
Figure 6. Second generation red OLED materials that are based on phosphorescent molecules.

Wang and co-workers reported on one of these methods by introducing aromatic amines to CN ligands of Ir(C−N)$_3$ complexes for red-shifting emission in 2007.[62] They showed that the pure red-emitting Ir-G1 complex, displayed in Figure 6, has a higher HOMO energy level and good morphological stability, achieving a maximum EQE of 11.65% and CIE color coordinates of (0.70, 0.30) in the OLED device. Larger π-electronic conjugation in the isoquinoline ring tuned the emission of Ir(III) complexes to the pure red spectral region (>620 nm). Furthermore, Kwon and co-workers used methyl groups and sterically bulky *tert*-butyl groups to suppress the self-quenching effect of [(phq)$_2$Ir(acac)] (phq = 2-phenylquinoline) complexes, which was reported in 2011.[63] A highly efficient red PhOLED based on the Ir(mphmq)$_2$(tmd) phosphor (see Figure 6) realized an EQE of 24.6% and an emission wavelength of 610 nm. In 2018, Wong and co-workers introduced the diarylboron group into heteroleptic Ir(III) complexes bearing ancillary acac ligands.[64] With the incorporation of a strong electron-deficient effect and the notable electron-transporting capacity of the diarylboron group, an up-to-date highest EQE value for Ir(III)-based red PhOLEDs using PyThIr (see Figure 6) over 28% with an emission wavelength of 604 nm was achieved.

The long-lived triplet states of platinum(II) complexes also favor the potential use in efficient red PhOLEDs with high color purity. In 2008, a red PhOLED utilizing terdentate Pt(II) complex PtL^{2}Cl, displayed in Figure 6, was successfully developed by Williams and co-workers. The resulting device exhibited an EQE of 14.5% at an emission peak of 700 nm.[65] By further optimization of materials and device architecture, Li and co-workers developed the tetradentate cyclometalated Pt(II) complex (PtN3N-ptb), which is depicted in Figure 6. PtN3N-ptb was

used as an emissive dopant in stable and efficient red OLEDs with long operational lifetimes of over 600 h at a luminescence of 1000 cd m^{-2}.[66] The maximum EQE of the red triplet emitter based on PtN3N-ptb, shown in Figure 6, can be improved to nearly 21.5%. In 2016, Chi and co-workers strategically designed and synthesized a new homoleptic Pt(fprpz)$_2$ complex (see Figure 6) with the intense near IR (NIR) emission at 740 nm and the PLQY of up to 81%.[67] The best NIR-emitting OLED with a peak EQE of 24 ± 1% was obtained for Pt(fprpz)$_2$ due to its high horizontal dipole orientation. Although some metal complexes derived from other transition elements, such as Re(I), Eu(III), and Zn(II), are known to exhibit monochromic red emissions, the use of these complexes for device applications is still limited because of their poor solubility and low luminescence efficiency.

3.2.3. Second Generation: Blue Emitters

In pursuit of high-performance electroluminescent OLED devices, phosphorescent emitters have drawn continuous attention. Iridium and platinum complexes are also suitable for blue phosphorescent emission. In 2001, the emitter FIrpic shown in **Figure 7** was first used by Forrest and co-workers to fabricate a blue phosphorescent OLED (CIE = 0.16, 0.29) with an EQE of 5.7% and the emission wavelength of 475 nm.[68]

Although many iridium complexes based on C^N ligands have shown high emission efficiency in the sky-blue region, designing deep-blue Ir(III) phosphors with a lower energy of the HOMO is desirable.[69] To achieve a blue-shift in the emission, the triplet energies have to be at least 2.8 eV.[70] The triplet energy can be increased by introducing electron-withdrawing

ADVANCED
SCIENCE NEWS
www.advancedsciencenews.com

ADVANCED
MATERIALS
www.advmat.de
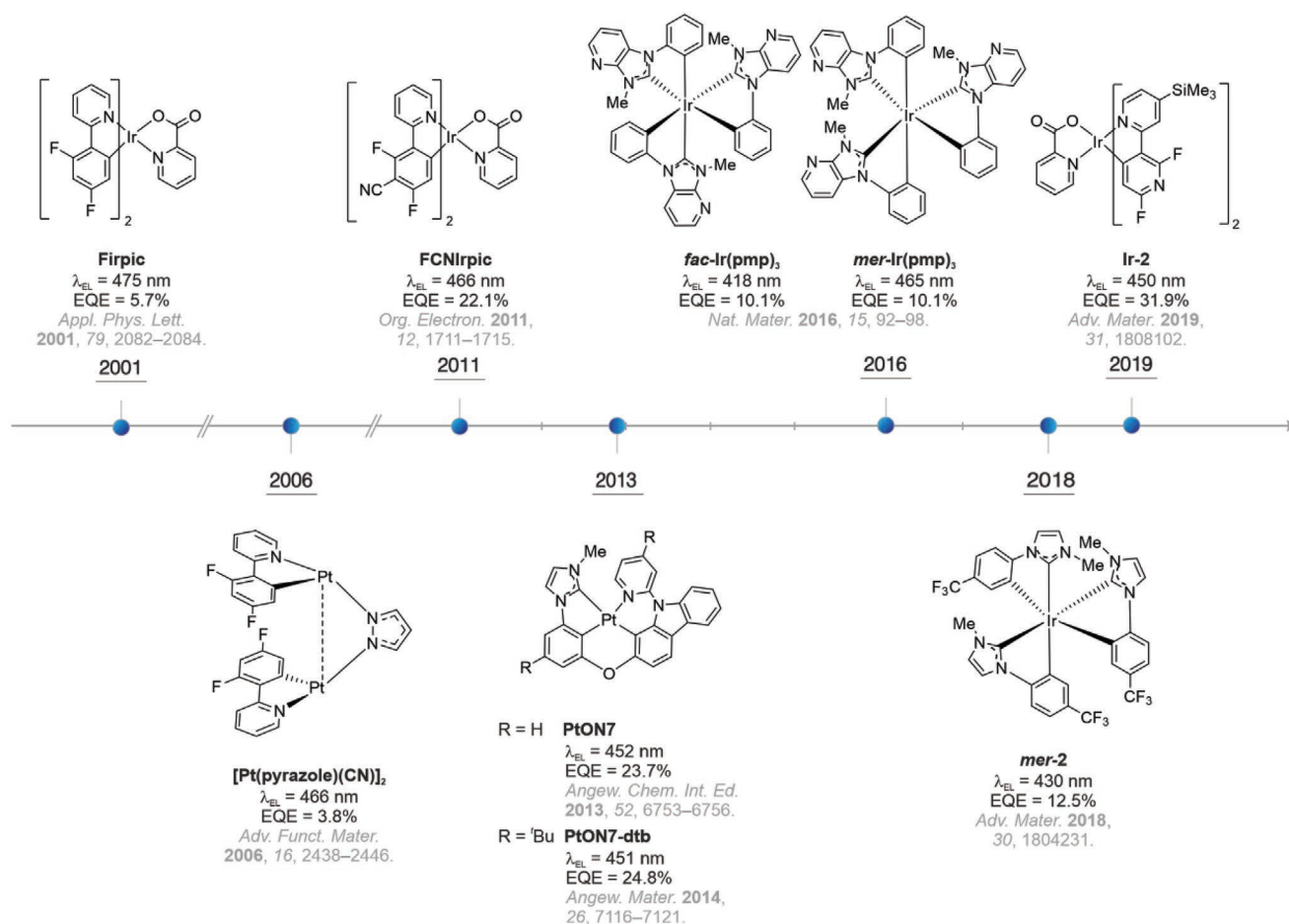
Figure 7. Second generation blue OLED emitters based on phosphorescent molecules.

groups. The attached nitrile group in FCNIrpic as shown in Figure 7, increases the triplet energy to 2.74 eV with an EQE of 22.1% and an emission wavelength of λ_{EL} = 466 nm in the OLED device.[71]

Many modified arylpyridine-type derivatives with different substituents and ancillary ligands have been designed to improve the color saturation of blue PhOLEDs.[70] A subsequent breakthrough was achieved by Forrest and co-workers who reported the fabrication of efficient blue PhOLEDs derived from (fac-) and (mer-)Ir(pmp)$_3$ complexes in 2016 as depicted in Figure 7.[72] Utilizing the σ-donating capabilities of N-heterocyclic carbene (NHC) ligands, these complexes can achieve deep blue emission (λ_{PL} = 418 nm) with decreased conjugation of the ligand scaffold. In particular, the fac-Ir(pmp)$_3$-based device achieved deep blue emission with color coordinates of (0.16, 0.09) with a very high brightness (>7800 cd m^{-2}), which is the brightest deep blue emission among the reported PhOLEDs. In 2018, Zysman-Colman and co-workers reported the meridional homoleptic Ir(III) complex mer-2 bearing the CF$_3$ substituted NHC ligands shown in Figure 7.[10b] Owing to the strong electron-withdrawing effect of meta-CF$_3$ group, mer-2 displayed a remarkable deep-blue emission at 412 nm with a PLQY of 72% in solution. The device using mer-2 achieved a high EQE of 12.5% at the brightness of 100 cd m^{-2}. In addition,

an extremely small CIE y-coordinate (< 0.1) was realized in the stable vacuum-deposited OLED.

In addition to the Ir-based complexes, platinum complexes are also well-established. In 2006, Thompson and co-workers reported upon a pyrazolate-bridged binuclear Pt(II) complex, [Pt(pyrazole)(CN)]$_2$ shown in Figure 7, that achieves an EQE of 4.3%, an emission wavelength of 466 nm, and CIE coordinates of (0.11, 0.24) in a blue OLED device.[73] Great improvement has been done in the development of Pt complexes with the introduction of the highly efficient rigid tetradentate Pt(II) complex PtON7 in 2013 and PtON7-dtb in 2014 by Li and co-workers as displayed in Figure 7.[74] The OLED devices containing the platinum(II) complex PtON7-dtb exhibited a pure deep-blue emission with an extremely narrow full width at half maximum (FWHM) of 20 nm. With an outstanding EQE of 24.8%, an EL wavelength of 451 nm, and CIE coordinates of (0.148, 0.079) in a PtON7-dtb-based OLED device, this emitter is one of the most promising deep blue phosphorescent platinum emitters.

Recently, Kim and co-workers reported a new series of dfpy-sipy-type Ir(III) complexes that show an outstanding intense blue emission with a narrow wavelength at λ_{PL} = 445–450 nm.[75] This work demonstrates the highest EQE = 31.9% of a deep blue device doped with Ir-2 (see Figure 7) among the reported PhOLEDs with a CIE y-coordinate less than 0.20.

**ADVANCED
SCIENCE NEWS**

www.advancedsciencenews.com

**ADVANCED
MATERIALS**

www.advmat.de
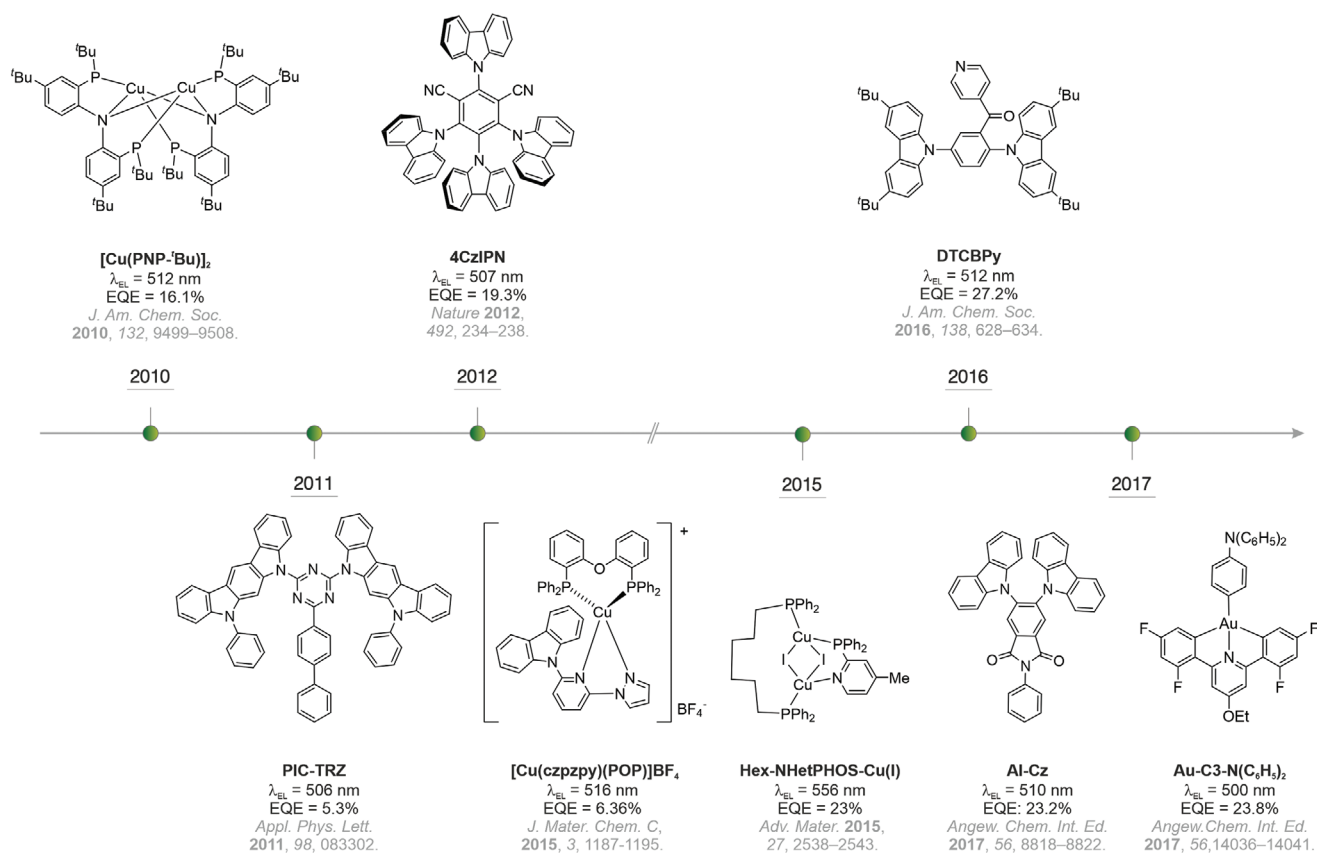
Figure 8. The third generation green OLED emitters is based on TADF molecules.

3.3. Third Generation Emitters

Although the emitters based on phosphorescent heavy-metal complexes have exhibited promising potential and have been employed in commercial electroluminescent products, the use of heavy-metal atoms limits their further market expansion considering the environmental concerns and cost issues.[7a] Thus, the development of emitters that avoid the usage of high-cost and environmentally precarious elements, while offering high IQEs has become an increasing motivation. One solution is the highly promising mechanism of TADF that has been developed. TADF is being investigated and utilized with increasing interest both in academia and industrial research. TADF molecules characteristically have a small energy gap (ΔE_{ST}) between the lowest-lying singlet state S_1 and lowest-lying triplet state T_1. When the lifetime of the T_1 excitons is long enough, the formally spin-forbidden reverse intersystem crossing (RISC) process is thermally activated and the triplet excitons can up-convert into the S_1 state through which they radiatively relax to the ground state which leads to a theoretical IQE of 100%.[76]

3.3.1. Third Generation: Green Emitters

In 2011, Adachi and co-workers introduced the first OLED using a purely organic TADF molecule as an emitter.[77] PIC-TRZ as

shown in **Figure 8** was built into an OLED device with an EQE of 5.3%, which approaches the theoretical limit of conventional fluorescent materials. Experimental data and quantum mechanical analysis suggest that the reduction in the overlap of HOMO and the lowest unoccupied molecular orbital (LUMO) reduced the energy gap ΔE_{ST} between S_1 and T_1, leading to a thermally activated reversibility of the ISC. Furthermore, Adachi and co-workers reported that a twisted donor and acceptor structure forced by steric hindrance, effectively reduces the overlap between HOMO and LUMO.

One year later, they succeeded in synthesizing a series of TADF emitters derived from carbazolyl dicyanobenzenes with multiple carbazolyl units as donor groups and benzonitriles as acceptor groups, marking a major milestone in TADF OLED emitter development.[78] An OLED featuring 4CzIPN (see Figure 8) as the emitter showed an excellent device performance with an outstanding EQE of 19.3% in comparison to OLEDs based on conventional fluorescent emitters which can only reach a maximum EQE of 5%, indicating that the emission process uses both singlet and triplet excitons through a highly efficient TADF mechanism.

In 2015, Cheng and co-workers reported a benzoylpyridine-carbazole-based emitter called DTCBPy as shown in Figure 8.[79] The emitter exhibited a small ΔE_{ST} value of 0.04 eV and a PLQY of 91.4% was observed when doped in a thin film. The respective green OLED device using DTCBPy

**ADVANCED
SCIENCE NEWS**

www.advancedsciencenews.com

**ADVANCED
MATERIALS**

www.advmat.de
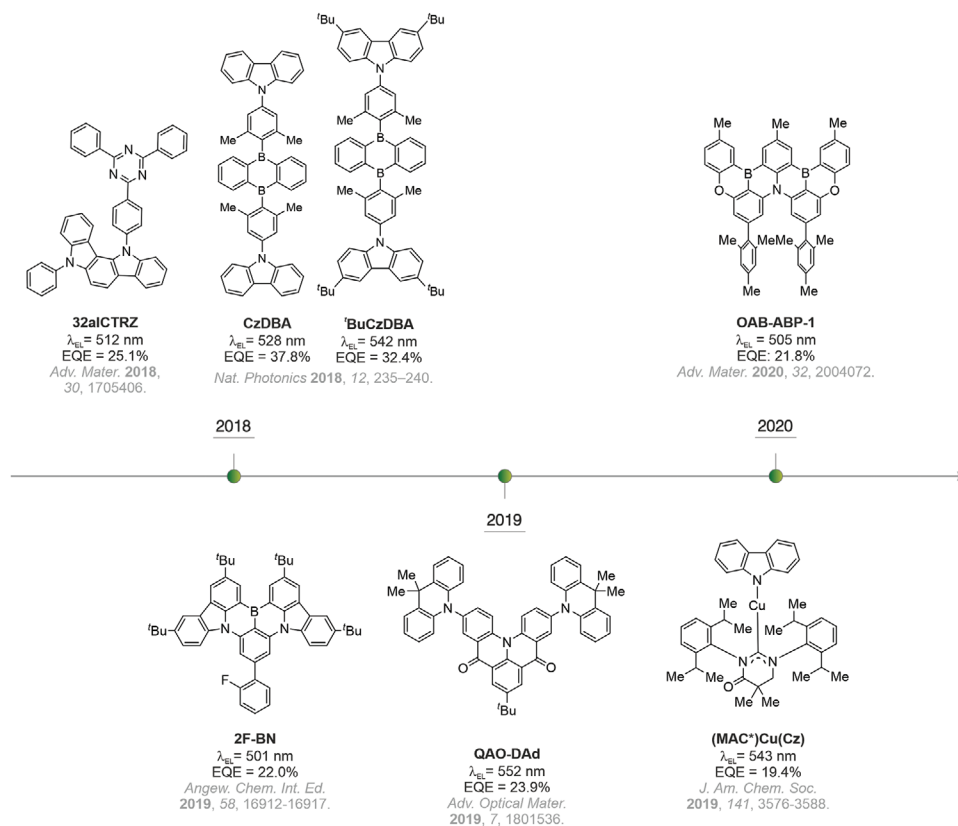
Figure 9. The third generation green OLED emitters are based on TADF molecules.

as the dopant emitter showed an EQE of 27.2%. The analysis of the crystal structure of DTCBPy indicates that the short distance of 2.9–3.7 Å between the *ortho-tert*-butyl carbazole unit (donor) and the pyridine group (acceptor) facilitated the strong intramolecular through-space interaction between the donor and acceptor moiety and that through-space interactions most likely play a key role to obtain very small ΔE_{ST} values simultaneous to high quantum efficiencies. In 2017, Chen and co-workers designed and synthesized an aromatic-imide-based TADF emitter AI-Cz shown in Figure 8, which showed delayed emission due to the small ΔE_{ST} (< 0.1 eV). Using this molecule as an emitter, excellent green OLED device with 510 nm and high EQE of 23.2%.[80]

In 2018, Duan and co-workers conducted studies on several TADF molecules derived from the indolocarbazole isomers as shown in **Figure 9**.[81] The emitter 32aICTRZ displayed excellent TADF properties in an OLED device with an EQE of 25.1%. In the same year, Cheng and co-workers reported two rod-like emitters, CzDBA and tBuCzDBA, that belong to the D–A–D type TADF molecules bearing 9,10-dihydro-9,10-diboraanthracene and carbazole groups as depicted in Figure 9.[82] These emitters show very small ΔE_{ST} in combination with high horizontal emission dipole orientations and excellent PLQYs. By using CzDBA as an emitter, a green OLED with a record-high EQE of 37.8% was achieved, which provides a new research direction to achieve highly efficient TADF-based OLEDs.

Recently, Duan and co-workers reported a novel TADF emitter 2F-BN displayed in Figure 9, based on the multi-resonance

design strategy, which can separate HOMO and LUMO effectively through the opposite resonance effect of a nitrogen atom and boron atom without the need of conventional donor-acceptor structures.[83] An excellent pure green device with an EQE of 22.0% and an FWHM of only 25 nm were realized. Enlighted by the above results, Jiang and co-workers designed and synthesized a new TADF emitter QAD-DAd shown in Figure 9 using a fused amine/carbonyl system. Employing QAD-DAd as emitter, highly efficient vacuum-deposited OLED with green emission (552 nm) and EQE of 23.9% were accessed.[84] Furthermore, Hatakeyama and co-workers reported a solution-processable OLED with the EQE of 21.8% and pure green emission of 505 nm, companied with an FWHM of 33 nm, through the use of the emitter OAB-ABP-1 which is depicted in Figure 9.[85] These excellent performances show the promising potential of a multi-resonance design strategy to construct TADF emitter for application in OLEDs.

Besides the purely organic TADF emitters, Cu(I) complexes with full-filled d^{10} shells have attracted considerable interest for their attractive photophysical properties. Since the first discovery of highly efficient green OLED prepared from a diamond core binuclear Cu(I) complex [Cu(PNP-tBu)]$_2$ with TADF properties, as shown in Figure 8, new copper complexes are emerging as TADF-emitting materials for OLEDs.[86] The homo- or heteroleptic Cu(I) complexes based on a butterfly-shaped Cu_2X_2 core bridged by an N,P-ligand, such as diphenylphosphinepyridine-derivatives (PyrPHOS), have received considerable attention as OLED candidates. The dinuclear

Cu_2X_2-unit in these compounds leads to a rigid structure compared to mononuclear complexes which causes improved photophysical properties (nearly 100% PLQY in solid-state). The solution-processed OLEDs based on heteroleptic copper–halide–(diphenylphosphino)pyridine derivatives (NHetPHOS) complex gave a maximum CE of 9 cd A^{-1} at a low turn-on voltage of 4.1 V in the yellow-to-green region.[87] To improve luminescent efficiency by enhancing molecular rigidity, 1,6-bis(diphenylphosphino)hexane was used instead of PPh_3 to get a fully bridged dicopper(I) complex Hex-NHetPHOS-Cu(I) (see Figure 8) which was reported by Bräse and co-workers in 2015.[88] It exhibited a very high PLQY of 92 ± 5% in solid films. High-efficiency solution-processed OLEDs were achieved with the largest CE of 73 ± 2 cd A^{-1} at an emission wavelength of 556 nm, corresponding to a peak EQE of 23 ± 1%. This represents the best efficiency of OLEDs based on green copper(I) complexes with TADF emission. Besides, many efforts on its bridging N,P-ligand, and terminal phosphine ligands have been devoted to addressing the effect of on the solubility, stability, and luminescence of $Cu_2X_2(NP)$ complexes.[89]

The cationic Cu(I) complexes $Cu(NN)(POP)^+$ can also be designed for green OLEDs via appropriate ligand engineering. In 2015, Lu and co-workers reported a brightly green $[Cu(czpzpy)(POP)]BF_4$ as displayed in Figure 8 by integrating the strong electron-donating carbazole moiety with the pypz unit.[90] The functional diimine ligand can not only be used in solution-processed OLEDs as a ligand to form the luminescent cuprous complex but also acts as a host for the formed emitter. A highly efficient green OLED with an emissive layer using $[Cu(czpzpy)(POP)]BF_4$ was fabricated with an EQE of 6.36% and current efficiency of 17.53 cd A^{-1}. Other d^{10} metal complexes, like Ag(I) and Au(I) complexes with low-lying MLCT or ligand-to-ligand charge transfer excited states were also found to possess TADF properties.[91] In 2017, Che and co-workers developed a series of luminescent cyclometalated Au(III) complexes with TADF character.[92] The presence of an amino substituent on the auxiliary aryl ligand twists for the C^N^C ligand plane and leads to the separation of HOMO and LUMO. The complex Au−C3−N(C_6H_5)$_2$ showed green EL (λ_{EL} = 517 nm) with a record-high maximum EQE of up to 23.8%.

Very recently, linear two-coordinate d^{10} coinage metal complexes have been developed as the most promising candidates for high-performance OLEDs. In 2016, Romanov and co-workers demonstrated two-coordinate, monomeric CAAC copper and gold halide complexes (CAAC)MX (CAAC = cyclic (alkyl)(amino)carbene, M = Cu, Au, X = Cl, Br, I) with high quantum efficiencies up to 95% and short lifetimes (about 0.5 ns) that exhibit prompt rather than delayed fluorescence.[93] Subsequently, several linear, trigonal, and dimeric CAAC coinage compounds bearing various co-ligands, for example, L = thiocyanate, 2,2′-bipyridine, phenanthroline, or the trispyrazolylborate derivatives, were also developed for exploring metal-based emitters.[94] Another remarkable progress on two-coordinate (carbene)Cu(N-carbazolyl) bearing monoamido aminocarbene (MAC*) and diamidocarbene (DAC*) has been successfully realized for efficient TADF emissions with near 100% IQE in full-color range varied over 270 nm.[95] The green device with (MAC*)Cu(Cz) (see Figure 9) as the dopant exhibited a maximum EQE of 19.4%, an emission wavelength of

534 nm, and high brightness of 54 000 cd m^{-2}. More recently, impressive efforts on the structure modification on (carbene) M(I)(amide) complexes, for example (carbene)Au(I)(amide), have been described to achieve efficient emitters with excellent electroluminescent properties.[96]

3.3.2. Third Generation: Orange-Red Emitters

The first orange-red emitter for third-generation OLEDs, 4CzTPN-Ph shown in **Figure 10**, was reported by Adachi and coworkers in 2012 with an EQE of 11.9% and an emitting wavelength of 580 nm.[78]

In 2013, the same group was able to introduce an OLED with a red-shifted emission (λ_{EL} > 600 nm) with an EQE of 17.5% and CIE coordinates (0.60, 0.40) featuring the heptazine-based emitter molecule HAP-3TPA shown in Figure 10 whose acceptor core was equipped with a higher number of heteroatoms.[97] In 2016, Monkman and co-workers introduced an OLED device containing a dibenzo[a,j]phenazine-based emitter belonging to U-shaped D-A-D TADF systems called POZ-DBPHZ as displayed in Figure 10 with an EL wavelength of 610 nm and EQE of 16%.[98] Ever since then, third-generation orange-red emitters have made considerable progress in recent years, leading to the development of TADF emitters that show luminescence in the region between 580 and 700 nm with EQEs up to ≈30%. In 2018, Yang and co-workers reported a device featuring NAIDPAC as the emitting dopant with an EL wavelength of λ_{EL} = 584 nm and an EQE of 29.2% as shown in Figure 10.[99] Their approach to increase the rigidity of the molecular structure, as well as a strongly pre-twisted charge transfer (CT) state, in combination with the contribution of the optical microcavity effect has led to high EQEs of this orange-red OLED system. Two years later, Cheng and co-workers reported an orange-red device containing the 9,10-diboraanthracene (DBA)-based, rod-like emitting dopant dmAcDbA shown in Figure 10 with an EQE of 24.9% and emission wavelength of 583 nm that featured methyl groups on the phenyl spacers which led to large torsion angles.[100]

While these devices showed exceptional EQEs, the emission wavelength was only in the orange-red region, opening space for the development of equally efficient purely red-emitting (>620 nm) OLED devices. One of the early deep-red OLED devices was reported by Wang and coworkers in 2015 when they implemented TPA-DCPP shown in Figure 10, a phenanthrene-based TADF emitter, into an OLED device showing EL with a wavelength of 668 nm and an EQE of 9.8%.[101] In 2019, Yang and co-workers reported a solution-processed device containing the follow-up model of their orange-red emitter NAI-DMAC, NAI_R3 shown in Figure 10 with an extended donor moiety using tert-butylbenzene groups, which emits at 622 nm and an EQE of 22.5%.[102] Their strategy of combining molecular engineering and host selection successfully increased the EQE for their OLED system. In the same year, Liao et al. reported a red OLED containing the luminophore TPA-PZCN (see Figure 10) with an EL wavelength of 628 nm and an EQE of 27.4%. Liao and coworkers also used increased structural rigidity as a design tool and improved the acceptor strength by suppressing the nonradiative transition by installing a large and planar

ADVANCED
SCIENCE NEWS

www.advancedsciencenews.com

ADVANCED
MATERIALS

www.advmat.de
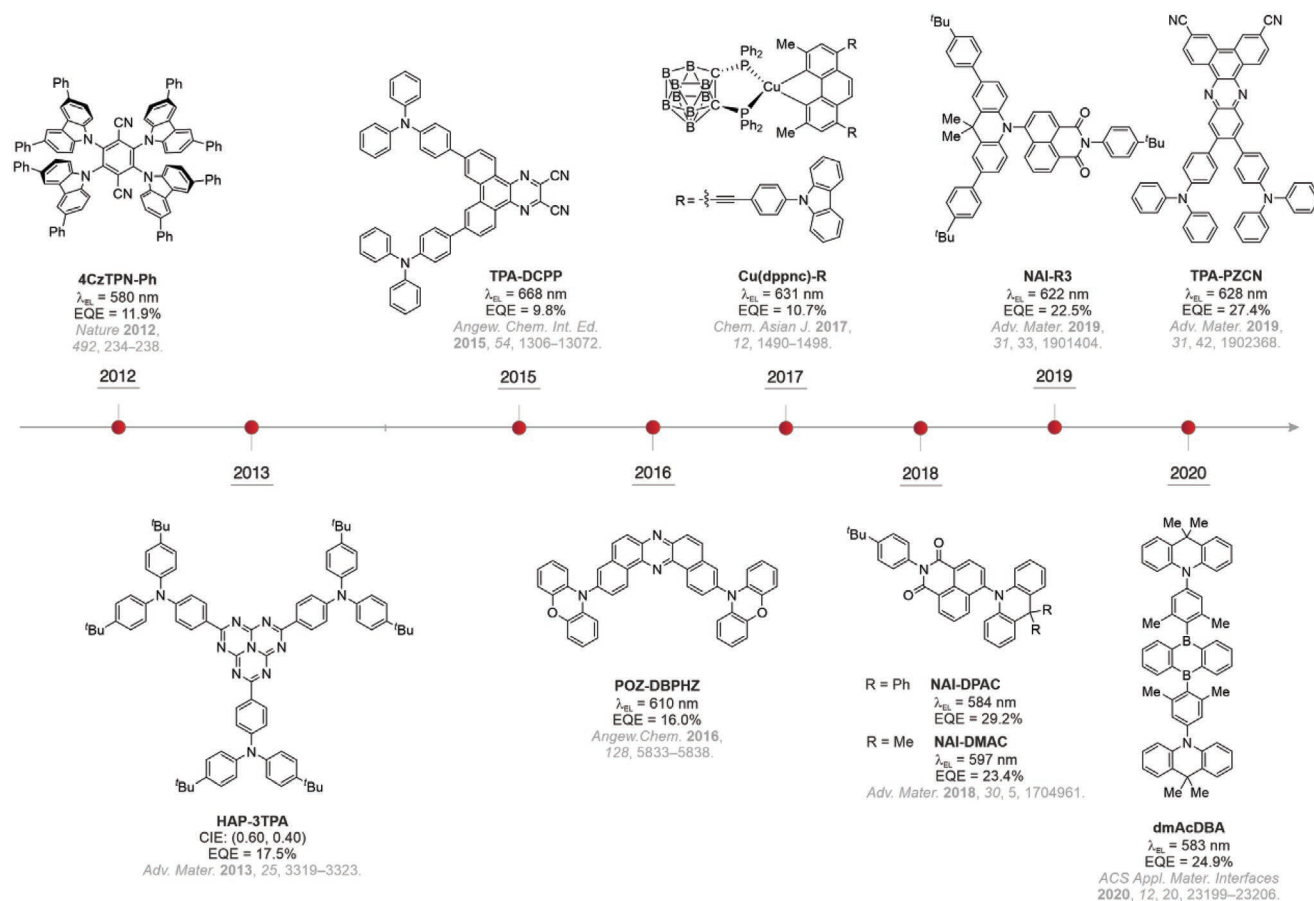
Figure 10. The third generation red OLED emitters are based on TADF molecules.

backbone.[103] Besides, the device performance was improved by using an exciplex-forming strategy which will not be discussed in detail at this point.

Purely organic orange-red third generation OLED devices started with a maximum EQE of 11.9% in 2012 and have evolved to reach record-high EQEs of almost 30% for deep-red devices in 2019. However, the spectrum of TADF emitters does not stop at red emitters. The progress on the development of NIR emitters with wavelengths above 700 nm is not the focus of this report and well-documented in previous reviews.[104]

Despite the efforts, the development of red TADF-based luminescent coinage complexes is still far behind because of their potential photosensitivity and limited luminescent properties which is following the energy gap law. Only a few red Cu(I)-based TADF compounds were reported to date.[105] In 2017, Che and co-workers proposed that by using an extended π-conjugation fragment in the complex Cu(dppnc)-R as displayed in Figure 10, a much larger oscillator strength (about 0.3) is obtained. The resulting red electroluminescent (λ_{EL} = 631 nm) device exhibited an EQE of up to 10.17% and CIE coordinates of (0.61, 0.38).[106]

3.3.3. Third Generation: Blue Emitters

Whilst the OLED devices based on first-generation emitters struggle with low EQEs, OLEDs containing second-generation

emitters achieved great success for red and green OLEDs. However blue OLEDs still face some series of challenges that come with the higher energy of blue light compared to red and green. This high energy leads to problems regarding the operation lifetime in blue OLEDs and too fast degradation of the material.[107] Furthermore, blue emitters are challenged by their high emission energy and extensive device efficiency roll-off at high brightness.[108] Therefore, the development of stable blue emitters and OLEDs, especially deep-blue, is one of the most challenging tasks in this research field.

In 2012, Adachi and co-workers published the very first class of deep-blue organic TADF emitters, the DTC-DPS as shown in **Figure 11**.[109] The OLED device equipped with DTC-DPS performed with an EQE of 9.9%, an EL wavelength of 423 nm, and CIE coordinates of (0.15, 0.07). Later that year, the group published a sky-blue emitter 2CzPN also displayed in Figure 11, which showed an EQE of 8% and an EL wavelength of 473 nm when built into an OLED device.[78] Since then, the evolution of blue TADF emitters has progressed rapidly. In 2014, Adachi and co-workers presented the next breakthrough in this research field.[110] They were the first to report a blue TADF OLED that was able to compete with the best phosphorescent OLEDs at that time. Furthermore, this was the first time that the issue of efficiency roll-off of blue OLEDs based on TADF was addressed. The TADF emitter of that OLED was based on a 9,10-dihydroacridine diphenylsulfone derivative DMAC-DPS

ADVANCED
SCIENCE NEWS
www.advancedsciencenews.com

ADVANCED
MATERIALS
www.advmat.de
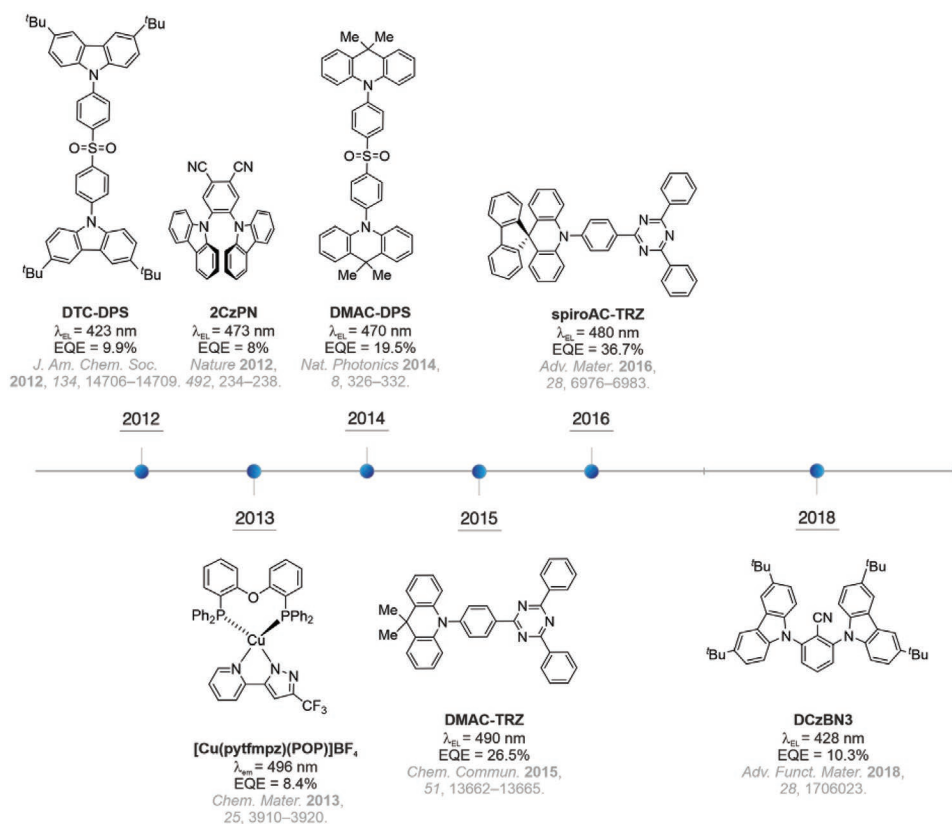
Figure 11. Selected third-generation blue OLED emitters based on TADF molecules.

as depicted in Figure 11. The device has a performance with an EQE of 19.5% with 470 nm and CIE coordinates of (0.16, 0.20). In 2015, Wu and co-workers published a new blue TADF emitter DMAC-TRZ as shown in Figure 11, which was counted to one of the best blue emitters at this time.[3,111] The respective OLED device performed with an EQE of 26.5%, an EL wavelength of 490 nm, and CIE coordinates of (0.21, 0.50). A structurally similar emitter to DMAC-TRZ, spiroAC-TRZ as depicted in Figure 11, was reported by Wu and co-workers in 2016.[112] The emitter spiroAC-TRZ is also based on a triazine acceptor and an acridine derivative donor. Compared to DMAC-TRZ, the phenyl rings on the acridine unit in spiroAC-TRZ weakens the electron-donating capacity of the donor. This weakening results in a favorable hypsochromic shift in the emission. The OLED device featured with spiroAC-TRZ performed with an EQE of 36.7% with 480 nm and CIE coordinates of (0.18, 0.43). With this high EQE, the OLED equipped with this emitter can be suggested as the best blue TADF device reported until 2017. Although, it is necessary to mention that the γ-coordinate CIE value of 0.43 is relatively large. In 2018, Adachi and co-workers presented a new TADF emitter DCzBN3, shown in Figure 11, based on a benzonitrile acceptor and two 3,6-di-tert-butylcarbazole donors.[113] The device with this emitter was the first deep-blue TADF OLED with a γ-coordinate below (0.07) and an EQE higher than 10%. The device performed with an EQE of 10.3%, an EL wavelength of 428 nm, and CIE coordinates of (0.16, 0.06).

In 2019, Cheng and co-workers reported the sky-blue TADF emitter 246tCzPPC, as depicted in **Figure 12**, which performed

in the device with an EQE of 29.6%, an EL wavelength of 491 nm, and CIE coordinates of (0.18, 0.40).[114] Another sky-blue TADF emitter with a high EQE was published in 2019 by Kido and co-workers.[115] The device with the emitter PXZ-BIP (see Figure 12) performed with an EQE of 20.1%, an EL wavelength of 497 nm, and CIE coordinates of (0.22, 0.42). Later in 2019, Yang and co-workers published the blue TADF emitter SBA2DPS as displayed in Figure 12, which performed in the respective OLED with an EQE of 25.5%, an EL wavelength of 467 nm, and CIE coordinates of (0.15, 0.20).[116] They stated that its high EQE is superior to most reported TADF devices with a CIE y-coordinate below (0.20).

Recently, in 2020, Zysman-Colman and co-workers designed and synthesized a molecule based on a fused amine/carbonyl system.[117] Due to the opposite resonance effect of a nitrogen and oxygen atom in Mes$_3$DiKTa (see Figure 12), the HOMO and LUMO were separated, resulting in a small ΔE_{ST} (0.26 eV). Excellent OLED device performance was realized with an EQE of 21.1%, sky-blue EL emission at 480 nm, and an FWHM of 37 nm. Another sky-blue TADF emitter was presented by Bräse and co-workers, who reported an OLED device containing the linear TADF molecule ICzTRZ, which displays a difunctionalized indolocarbazole core (see Figure 12). This emitter showed a PLQY of 70% and a highly horizontally oriented feature in host materials, which lead to an excellent device performance with an EQE of 22.1%, EL emission wavelength at 483 nm, and CIE coordinates of (0.17, 0.32).[118] Also this year, Tang and co-workers reported a series of TADF emitters based on

**ADVANCED
SCIENCE NEWS**

www.advancedsciencenews.com

**ADVANCED
MATERIALS**

www.advmat.de
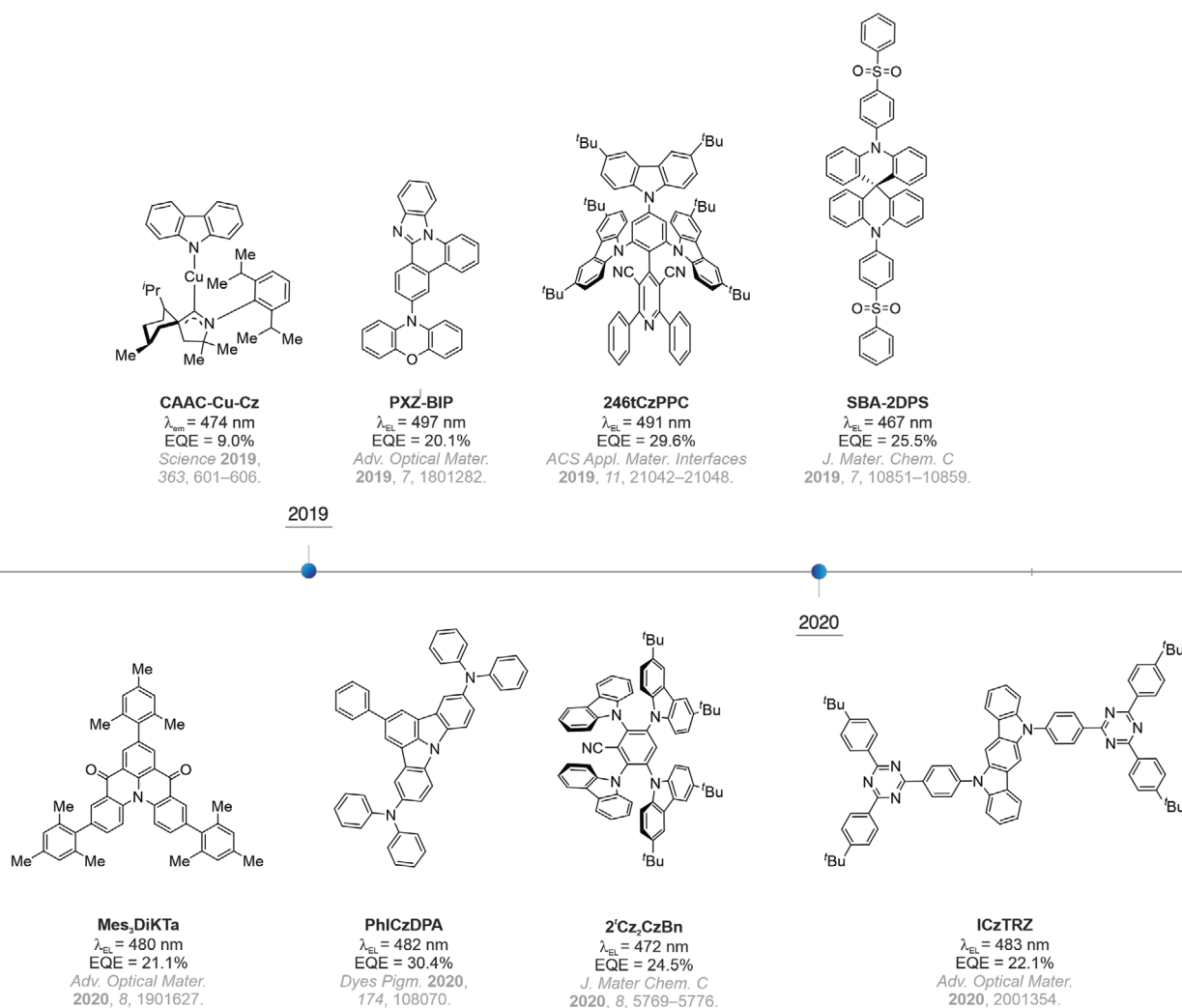
Figure 12. A selection of third-generation blue OLED emitters based on TADF molecules.

benzonitrile derivatives.[119] These emitters bear both 3,6-di-*tert*-butylcarbazole and carbazole as donor moieties and differ in their arrangement of the donors. The OLED device with 2^{t}CZ$_2$CzBn performed with an EQE of 24.5%, an EL wavelength of 472 nm, and CIE coordinates of (0.16, 0.24) as displayed in Figure 12. Lee and co-workers achieved an even higher EQE of 30.4% in an OLED employing the TADF emitter PhICzDPA as shown in Figure 12.[120] The device showed a sky-blue emission at 482 nm and CIE coordinates of (0.13, 0.32). The emission is located in the sky-blue region due to the strong donor character of the diphenylamine donors.

Besides the purely organic TADF emitters, there have been efforts to develop Cu(I)-based blue TADF emitters. In 2013, Lu and co-workers reported the blue-emitting cationic cuprous complex [Cu(pytfmpz)(POP)]BF$_4$ containing the electron-rich pypz ligand as visualized in Figure 11.[90] An intense blue TADF emission with λ_{PL} at 492 nm with a PLQY up to 75% was observed. Solution-processed blue OLEDs were fabricated. By using this emitter as dopant, a maximum EQE of 8.4%, an emission wavelength of 496 nm, and an excellent efficiency of 23.68 cd A^{-1} were achieved. However, the ionic Cu(I) complexes

still suffer the high roll-off effect in OLEDs caused by the interference of free counterions. Recently in 2019, Thompson and co-workers proposed a linear donor-bridge-acceptor design strategy and developed a new class of two-coordinate CAAC-Cu-amide complexes.[121] As a consequence of the strong ISC manifold within the coplanar ligand conformation, the smallest ΔE_{ST} values (<75 meV) in CAAC-Cu-amide complexes was observed for mononuclear Cu(I)based TADF systems. The resulting blue OLED employing CAAC-Cu-Cz as depicted in Figure 12 showed an EQE of 9%, a λ_{EL} of 474 nm and a power efficiency of 16 cd A^{-1} at 2 mA cm^{-2}.

3.4. Fourth Generation OLEDs–Next-Generation Emitter Development

However, the development of OLEDs does not end at devices based on third-generation emitters. The next generation of OLED devices needs to show good efficiencies, color purity, and long lifetimes amongst other factors. Several approaches are investigated to further improve the device efficiencies by

**ADVANCED
SCIENCE NEWS**

www.advancedsciencenews.com

**ADVANCED
MATERIALS**

www.advmat.de
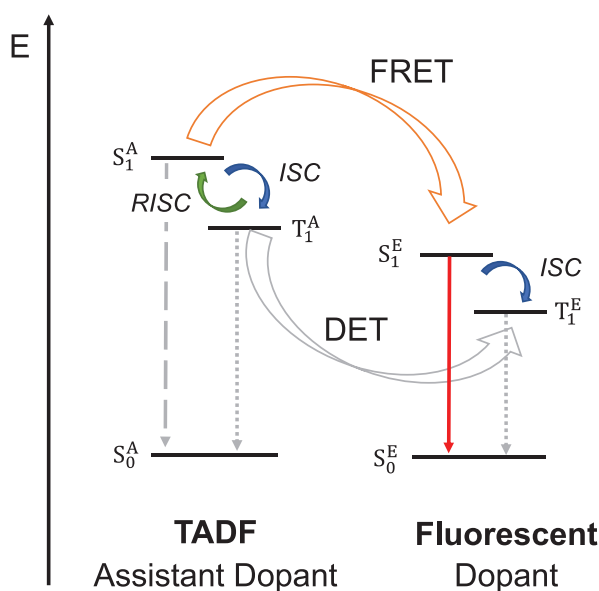
Figure 13. Simplified schematic outline of the main energy transfer and luminescence pathways taking place in hyperfluorescent devices, red-colored lines: pathways taking part in fluorescence and hyperfluorescence, grey-colored: unwanted (non-)radiative decays, Index explanation: A–assistant dopant, E–emitter.

optimizing the exciton harvesting. Here, we briefly introduce further developed luminescence pathway concepts for OLEDs based on fluorescence. Outside the fluorescence pathways, innovative phosphorescence-based concepts have also been explored and reported.[58,122]

Recently, in 2019, Endo and co-workers from Kyulux reported upon hyperfluorescence which they claim as the "ultimate solution for OLED displays".[123] "Hyperfluorescence" is a term that has been circulating in the world of OLEDs since 2013 and can also be found as "thermally assisted fluorescence" amongst other labels.[124] Since 2014, it is used to describe the use of TADF molecules as assistant dopants to a fluorescent emitter as reported by Adachi and co-workers.[125] The group reported an OLED device featuring cascade-type EL that was based on the combination of an emitter and assistant dopant in the EML. By regulating the doping concentration ratio of the TADF assist dopant and fluorescence emitter, the main exciton formation is localized on the assistant molecules. There, through TADF, the formed triplet excitons are upconverted via RISC into the S_1^A state (see **Figure 13**). Subsequently, the S_1^A exciton energies are transferred to the S_1^E state of the emitter molecule by Förster resonance energy transfer (FRET). The delayed fluorescence emitted from S_1^E results in the emission of light. This concept profits both from the high stability and narrow emission spectra of fluorescent emitters and thus, high color purity, as well as the efficient RISC process of TADF molecules that allows for a theoretical 100% exciton use to get high device efficiencies.

In 2014, a blue, green, yellow, and red hyperfluorescent OLED was reported by Adachi and co-workers.[125] The yellow device containing PXZ-TRZ as an assistant dopant with TADF characteristics and DBP as a fluorescent emitter in the EML (see **Figure 14**) showed the best maximum EQE of 18.0% with

the CIE coordinates (0.45, 0.53). Five years later, the hyperfluorescent devices by Endo and co-workers from Kyulux showed impressive performances.[123] Their blue, green, yellow, and red hyperfluorescent devices showed very narrow emission spectra, which resulted in higher color purity, significantly higher light intensities in comparison with phosphorescence and TADF-based OLEDs and long lifetimes. Their blue device achieved a maximum EQE of 26% with an EL wavelength of 470 nm, CIE coordinates of (0.14, 0.15), and an FWHM of 31 nm.

In 2018, Lee and co-workers reported upon an OLED device with a sequentially deposited sensitizer-doped EML and fluorescent emitter-doped EML containing DMAC-DPS as a TADF sensitizer dopant and TBPe as the fluorescent emitter as shown in Figure 14.[126] The multilayered EML structure that they reported allowed for the spatial separation of the two components of the emitting system which led to the suppression of the Dexter energy transfer (DET) that competes with the FRET (see Figure 13). Thereby, the FRET process was favored and the maximum EQE of the blue multilayered stacked sensitizer device improved by ≈5% in comparison to the conventional sensitizer device to 18.8% with CIE coordinates of (0.14, 0.25). In the same year, the same group reported on a solution-processed hyperfluorescent blue OLED device with an EML also using TBPe as the fluorescent emitter but 5CzCN as a TADF assistant dopant and a sterically more demanding host material as shown in Figure 14. The OLED displayed a maximum EQE of 19.5% with CIE coordinates of (0.15, 0.23).[127] Lee and co-workers furthermore reported on a molecular design option of the TADF assistant dopant to manage DET in a green hyperfluorescent device in 2018.[128] In their device, they used TbCzTrz as the TADF assistant dopant and 6tBPA as the fluorescent emitter (depicted in Figure 14). By increasing the steric demand of the TADF donor moiety with the addition of tert-butyl groups, the efficiency loss via DET could be successfully controlled. The resulting OLED device showed an EQE of 18.5% and CIE coordinates of (0.25, 0.57).

One year later in 2019, Kasparek, Baumann, and coworkers from CYNORA discussed methods to match TADF and fluorescent emitters for a co-emitting approach which is to be applied in deep-blue hyper OLED devices, further endorsing the hyperfluorescent concept from the side of the industry.[129] They reported on a hyperfluorescent OLED device with an EQE of 20%, which is less than for the traditional TADF-based device (24%), but with an improved CIEy coordinate (0.13) and longer lifetime at 1 000 cd m^{-2} (25 h). They conclude that the choice of the TADF versus the hyperfluorescent approach is to be determined by the application and the panel maker's requirements and that the matching of the TADF emitter and co-emitter is essential to a successful co-emitting approach. This is supported by a report by van Eersel and co-workers from 2019 when they simulated the efficiency loss processes in hyperfluorescent OLEDs in a Monte Carlo (MC) simulation and highlighted the importance of the optimization of the energy levels of the fluorescent emitter to those of the TADF emitter and host material, next to the doping concentration of the fluorescent emitter.[130] In the same year, another report on a MC simulation was published by Howard and co-workers, in which they state that the concept of hyperfluorescence might be instrumental to whether TADF molecules will be able to outcompete phosphorescent
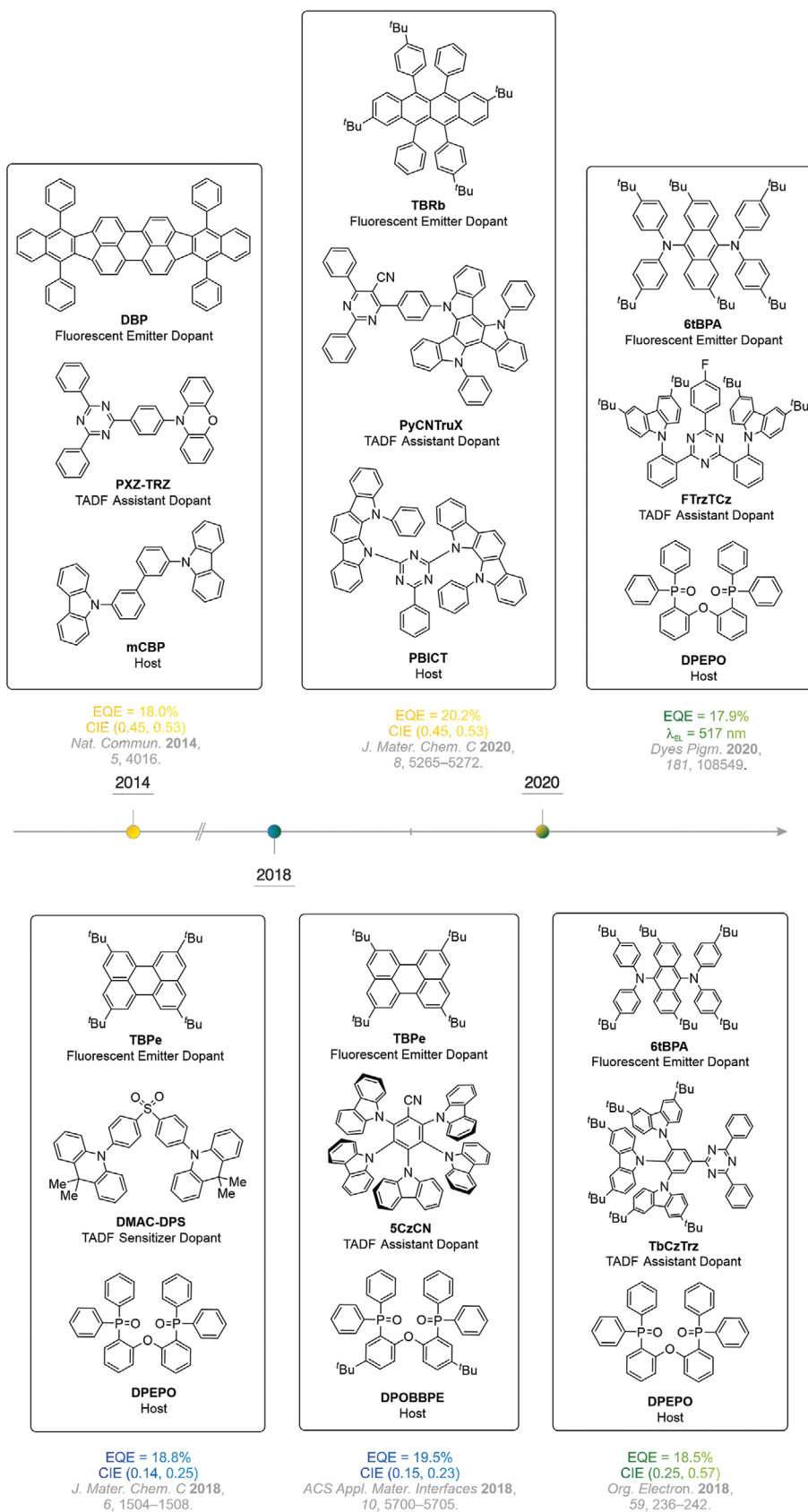
Figure 14. A brief timeline of the development of hyperfluorescent OLEDs showing a selection of device EMLs.

**ADVANCED
SCIENCE NEWS**

www.advancedsciencenews.com

**ADVANCED
MATERIALS**

www.advmat.de
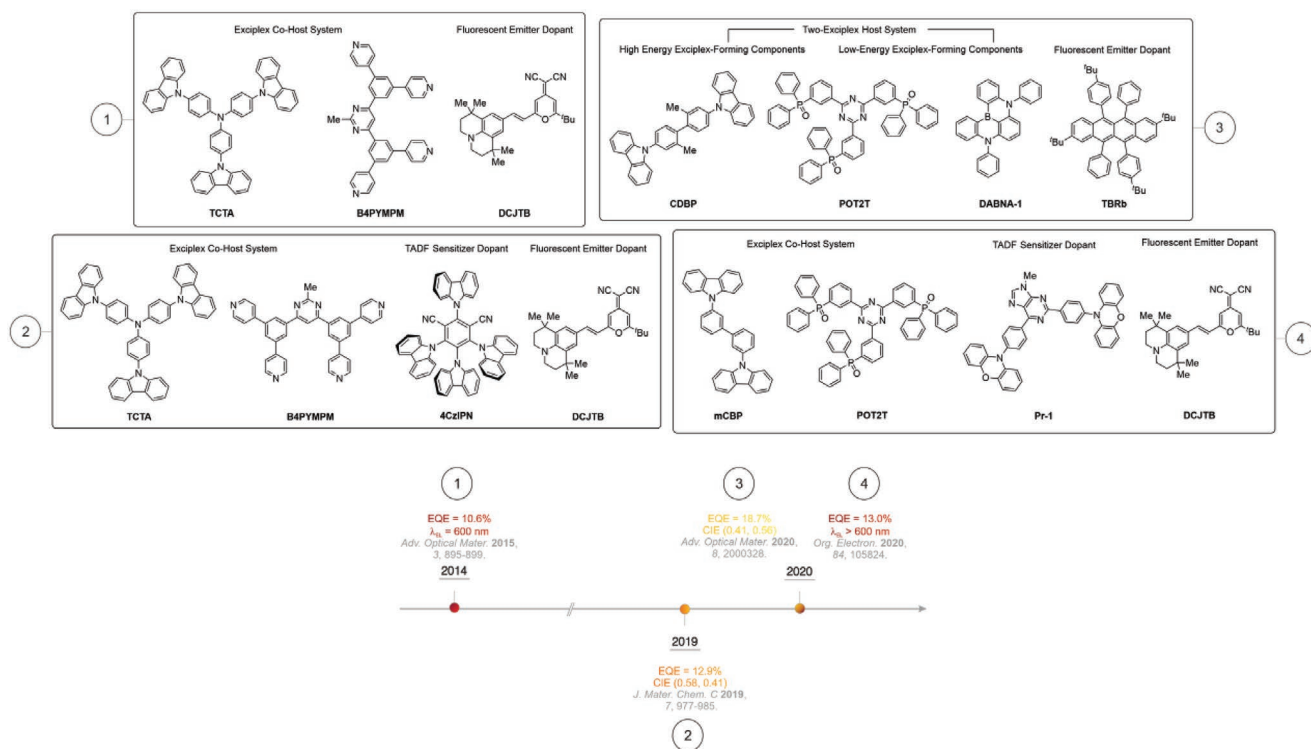
Figure 15. A brief timeline of the selected OLED EML systems using TADF-based systems in combination with fluorescent molecules.

emitters in OLEDs.[131] They investigated the singlet and triplet exciton diffusion lengths for TADF molecules and how they affect the efficiency of hyperfluorescence. Their study suggested two pathways toward high-efficiency hyperfluorescence: i) steric protection of the fluorescent acceptors to suppress triplet exciton-based DET and ii) limitation of triplet exciton mobility between TADF molecules.

Most recently, in 2020, Lee and co-workers reported upon a yellow TADF-sensitized fluorescent OLED (FOLED) that displayed a high EQE of 20.2%, CIE coordinates of (0.45, 0.53), and a lifetime of 1 400 h.[132] They used PyCNTruX as the TADF assistant dopant and TBRb as the fluorescent emitter dopant as shown in Figure 14. The combination of a small ΔE_{ST} that accelerated RISC and a bulky donor moiety led to higher EQEs and a long lifetime due to the suppressed DET. Furthermore, in the same year, the group published a green hyperfluorescent OLED that employed FTrzTCz as the TADF assistant dopant and 6tBPA as the fluorescent dopant with an EQE of 17.9%, CIE coordinates of (0.24, 0.58), and an EL wavelength of 517 nm as displayed in Figure 14.[133] Here, the DET was successfully reduced by installing sterically demanding *tert*-butyl groups and a largely distorted structure of the TADF emitter. In both reports, Lee and co-workers were able to improve their device performance by adjusting the steric demand of the donor moiety of the TADF molecule which is to their finding from 2018.

Simultaneous to the development of hyperfluorescent devices, other systems based on the combination of TADF-based systems and fluorescent molecules were investigated.

In 2015, Kim and co-workers reported a red FOLED using an exciplex-forming co-host system, deploying TCTA and B4PYMPM, and the fluorescent dopant DCJTB, shown in

Figure 15, with an EQE of 10.6% and EL at 600 nm that harvested triplet excitons by a RISC of the host triplet exciplex as depicted in **Figure 16**.[134]

In 2019, Liao and co-workers reported upon an orange FOLED that introduced a three-component EML as shown in Figure 15 containing i) an exciplex-forming co-host system consisting of one hole- and one electron-transporting material (TCTA, B4PYMPM), ii) a TADF dopant (4CzIPN) that acts as
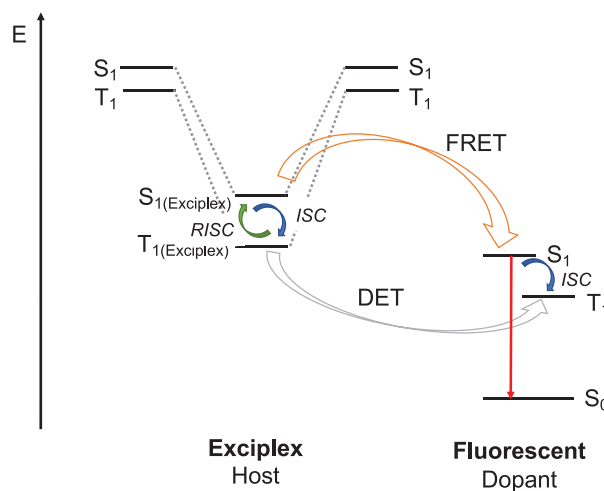
Figure 16. Simplified schematic outline of the exciplex-forming co-host system as reported by Kim and co-workers in 2015.[134] (Non-)radiative (decay) pathways that are not essential to the explanation of the luminescence pathway of the above-mentioned device are not depicted due to reasons of overview and comprehensibility.

**ADVANCED
SCIENCE NEWS**

www.advancedsciencenews.com

**ADVANCED
MATERIALS**

www.advmat.de
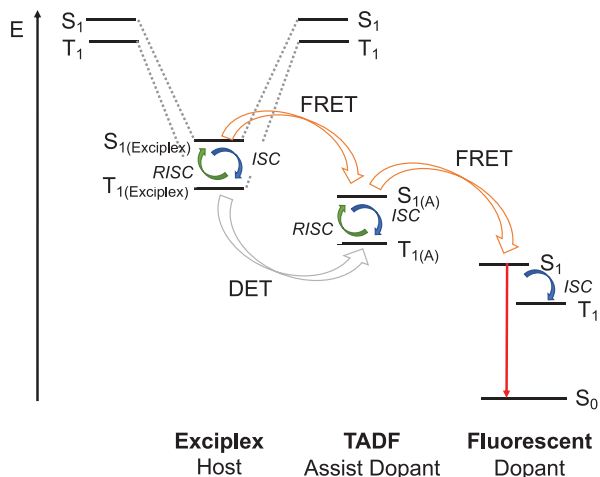
Figure 17. Simplified schematic outline of the exciplex-forming co-host hyperfluorescent system as described by Liao and co-workers in 2019.[135] (Non-)radiative (decay) pathways that are not essential to the explanation of the luminescence pathway of the above-mentioned device are not depicted due to reasons of overview and comprehensibility.

a sensitizer, and iii) a fluorophore (DCJTB) as schematically displayed in **Figure 17**.[135] Hereby, the exciplex-forming co-host system is the crucial theoretical concept of realizing hyperfluorescence. The highest EQE for the investigated OLEDs was 12.9% with CIE coordinates of (0.58, 0.41).

In 2020, Lee and co-workers introduced a cascade singlet-harvesting (CSH) OLED that uses a singlet-harvesting matrix which is doped with a fluorescent emitter as schematically displayed in **Figure 18**.[136] The singlet-harvesting matrix features two TADF-type exciplexes – the high energy exciplex and the low energy exciplex – that efficiently harvest excitons through the reverse ISC and lead to singlet exciton transfer to the fluorescent emitter through two FRETs while controlling the DET exciton loss mechanism. The high energy exciplex is formed by CDBP and POT2T, while the low energy exciplex is generated by POT2T and DABNA-1 (see Figure 14). The yellow OLED
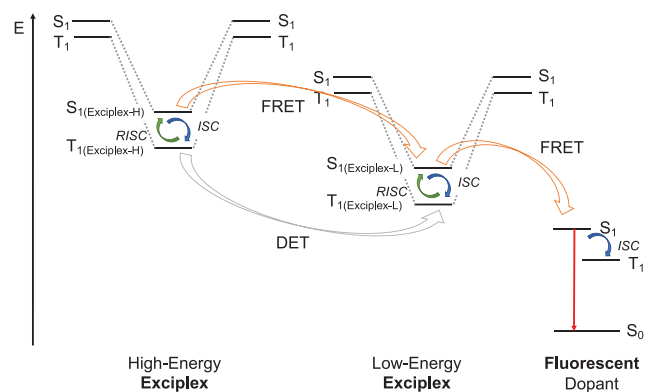
Figure 18. Simplified schematic outline of the CSH mechanism as described by Lee and co-workers in 2020.[136] (Non-)radiative (decay) pathways that are not essential to the explanation of the luminescence pathway of the above-mentioned device are not depicted due to reasons of overview and comprehensibility.
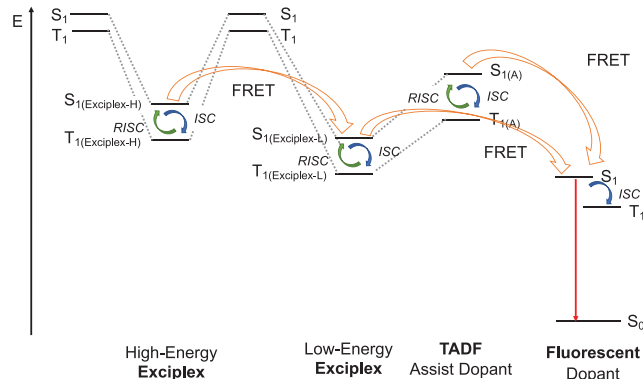
Figure 19. Simplified schematic outline of the cascaded energy transfer process in FOLED devices as reported by Ma and co-workers in 2020.[137] (Non-)radiative (decay) pathways that are not essential to the explanation of the luminescence pathway of the above-mentioned device are not depicted due to reasons of overview and comprehensibility.

device with the fluorescent emitter dopant TBRb presented a maximum EQE of 18.7%. with CIE coordinates of (0.41, 0.56).

In 2020, Ma and co-workers reported upon a red OLED device featuring an EML with an exciplex host (mCBP, POT2T), a TADF sensitizer (Pr-1) that also formed a low-energy exciplex with the electron-acceptor component (POT2T) from the exciplex host and a fluorescent emitter (DCJTB) as depicted in Figure 15 and schematically outlined in **Figure 19**.[137] The red OLED device of Ma and co-workers achieved a maximum EQE of 13.0% and EL wavelengths above 600 nm.

In 2018 and 2019, Yersin and co-workers stated the direct singlet harvesting (DSH) mechanism as a promising lead toward fourth-generation OLEDs.[138] The DSH mechanism tackles the search for better OLED EML materials from a slightly different direction. Instead of using TADF in combination with fluorescence, they propose the improvement of exciton use by introducing the follow-up step from TADF. They eliminate the need for time-delaying thermal activation to up-convert triplet excitons into a singlet state and accelerate ISC that directs singlet and triplet excitons directly into the lowest-lying singlet state (^{1}CT). The focus point of DSH is an almost "zero-gap" energy between the lowest-lying singlet state ^{1}CT and triplet state ^{3}CT that leads to fast ISC as depicted in **Figure 20**.

In summary, OLED development is ever-evolving and finding innovative ways to improve device performance and lifetime. Most recently, in April 2020, Kyulux announced that
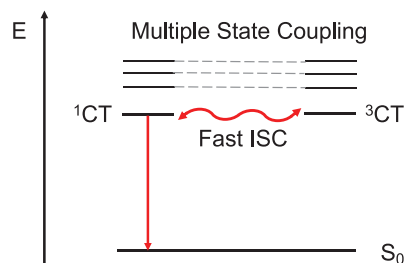
Figure 20. Simplified schematic outline of the DSH mechanism as reported by Yersin and co-workers.[138b]

**ADVANCED
SCIENCE NEWS**

www.advancedsciencenews.com

**ADVANCED
MATERIALS**

www.advmat.de

it had begun shipping a yellow TADF/Hyperfluorescence light-emitting material to Wisechip Semiconductor Inc. (Taiwan), marking the first commercialization of hyperfluorescent emitters to the best of our knowledge.[26]

4. Conclusion

In conclusion, the development of OLEDs and especially the emitting materials have come a long way ever since the pioneering work of Tang et al. in 1987.[33] Since then, we have seen the evolution of first-generation fluorescent emitters to second-generation phosphorescent emitters toward increased efforts to build third-generation devices based on TADF luminophores which allow for IQEs up to 100% by accessing both singlet and triplet excitons via RISC. Green, orange-red, and blue devices with a wide range of color and efficiencies have been introduced in all three generations based on emitting materials that are either metal-based or purely organic. Now, next-generation emitting materials are fast-emerging and convincing both academia and industry that the history of OLED development has yet another season of even better devices coming.

Among the various approaches to innovation in the OLED technology, one strategy to further improve the light-output of OLED devices is the usage of well-ordered structures like (surface-mounted) metal-organic frameworks (SUR)MOFs to tune the electron-hole mobility.[139] The first MOF showing TADF was reported in 2018 by Adachi and co-workers.[140] Very recently, a SURMOF-based OLED device with a green-emitting TADF molecule was built by Wöll and co-workers.[141] The SURMOF approach improved the charge transport of the OLED significantly due to reduced defects and a high-quality interface between SURMOF and the transport layer. Therefore, SURMOFs should be considered for future stack architectures of OLED devices. A different approach to innovation uses luminophores that intrinsically emit circularly polarized light to achieve higher brightness of OLEDs, and a simplified and thinner OLED device architecture.[142] Compared to non-polarized OLEDs built with antiglare filters to reduce external reflection, Fuchter and co-workers reported an improved brightness of 19% by employing a helical-chiral platinum complex.[143] Twist-induced TADF OLED emitter materials showing planar chirality were developed by Bräse and co-workers who reported circularly polarized luminescence enabled chiral molecules based on a carbazolophane (Czp) donor unit for the potential application in circularly polarized OLEDs.[144]

Conflict of Interest

The authors declare no conflict of interest.

[1] A. Arjona-Esteban, D. Volz, in *Highly Efficient OLEDs*, Wiley-VCH Verlag GmbH & Co. KGaA, Weinheim, Germany **2018**, p. 543.

[2] Y. Takahashi, Y. Furuki, S. Yoshida, T. Otani, M. Muto, Y. Suga, Y. Ito, *Dig. Tech. Pap. — Soc. Inf. Disp. Int. Symp.* **2014**, *45*, 381.

[3] M. Y. Wong, E. Zysman-Colman, *Adv. Mater.* **2017**, *29*, 1605444.

[4] N. Thejo Kalyani, S. J. Dhoble, *Renewable Sustainable Energy Rev.* **2015**, *44*, 319.

[5] M. Aleksandrova, *Adv. Mater. Sci. Eng.* **2016**, *2016*, 4081697.

[6] a) C. Bizzarri, E. Spuling, D. M. Knoll, D. Volz, S. Bräse, *Coord. Chem. Rev.* **2018**, *373*, 49; b) X. Yang, G. Zhou, W. Y. Wong, *Chem. Soc. Rev.* **2015**, *44*, 8484.

[7] a) D. Volz, M. Wallesch, C. Flechon, M. Danz, A. Verma, J. M. Navarro, D. M. Zink, S. Bräse, T. Baumann, *Green Chem.* **2015**, *17*, 1988; b) H. Yersin, *Highly Efficient OLEDs with Phosphorescent Materials*, Wiley-VCH Verlag GmbH & Co. KGaA, Weinheim, Germany **2007**; c) J. Shinar, *Organic Light-Emitting Devices*, Springer, New York, NY, USA **2004**.

[8] M. Godumala, S. Choi, M. J. Cho, D. H. Choi, *J. Mater. Chem. C* **2016**, *4*, 11355.

[9] M. Godumala, S. Choi, M. J. Cho, D. H. Choi, *J. Mater. Chem. C* **2019**, *7*, 2172.

[10] a) C. Fu, S. Luo, Z. Li, X. Ai, Z. Pang, C. Li, K. Chen, L. Zhou, F. Li, Y. Huang, Z. Lu, *Chem. Commun.* **2019**, *55*, 6317; b) A. K. Pal, S. Krotkus, M. Fontani, C. F. R. Mackenzie, D. B. Cordes, A. M. Z. Slawin, I. D. W. Samuel, E. Zysman-Colman, *Adv. Mater.* **2018**, *30*, 1804231.

[11] a) Q. Wei, Z. Ge, B. Voit, *Macromol. Rapid Commun.* **2019**, *40*, 1800570; b) C. Cole, S. Kunz, N.-P. Thoebes, P. M. Sonar, J. Blinco, C. Barner-Kowollik, S. D. Yambem, *Organic and Hybrid Light Emitting Materials and Devices XXIV* (Eds: C. Adachi, J.-J. Kim, F. So), SPIE, San Diego **2020**.

[12] C. A. Parker, C. G. Hatchard, *Trans. Faraday Soc.* **1961**, *57*, 1894.

[13] M. Pope, P. Magnante, H. P. Kallmann, *J. Chem. Phys.* **1963**, *38*, 2042.

[14] M. Koden, *OLED Displays and Lighting*, John Wiley & Sons, New York **2016**.

[15] S. A. VanSlyke, C. W. Tang, L. C. Roberts, (Eastman Kodak Co), USA US4720432A, **1987**.

[16] a) *OLED history: A 'guided tour' of OLED highlights from invention to application*, https://www.oled-info.com/history, accessed: May, **2020**; b) R. Mertens, *The OLED Handbook – A Guide to OLED Technology*, Industry & Market, **2019**; c) T. Tsujimura, *OLED Display Fundamentals and Applications*, Wiley, **2017**.

[17] R. M. T. Wakimoto, K. Nagayama, Y. Okuda, H. Nakada, T. Tohma, *1996 SID International Symp.*, SPIE, San Diego **1996**.

[18] a) J. H. Burroughes, D. D. C. Bradley, A. R. Brown, R. N. Marks, K. Mackay, R. H. Friend, P. L. Burns, A. B. Holmes, *Nature* **1990**, *347*, 539; b) M. Fleuster, M. Klein, P. v. Roosmalen, A. d. Wit, H. Schwab, *Dig. Tech. Pap.— Soc. Inf. Disp. Int. Symp.* **2004**, *35*, 1276.

**ADVANCED
SCIENCE NEWS**
www.advancedsciencenews.com

**ADVANCED
MATERIALS**
www.advmat.de

[19] J. W. Hamer, A. Yamamoto, G. Rajeswaran, S. A. Van Slyke, *Dig. Tech. Pap.— Soc. Inf. Disp. Int. Symp.* **2005**, *36*, 1902.

[20] a) R. M. A. Dawson, M. G. Kane, *Dig. Tech. Pap.— Soc. Inf. Disp. Int. Symp.* **2001**, *32*, 384; b) B. Santo, *The Consumer Electronics Hall of Fame: Nokia N85 Cellphone*, https://spectrum.ieee.org/consumer-electronics/gadgets/the-consumer-electronics-hall-of-fame-nokia-n85-cell-phone, accessed: October, **2020**; c) N. John, *Samsung I7110 with OLED screen officially announced*, http://nokiaworld.org/1001-samsung-i7110-with-oled-screen-officially-announced/ accessed: October, **2020**.

[21] a) *Lumiotec to Market Two OLED Luminaires – World First in Mass-produced Models*, http://www.lumiotec.com/en/news/pdf/20110727_lumiotecnewsrelease_eng.pdf, accessed: October, **2020**; b) S. Corporation, *2007: Sony Launches World's First OLED TV*, https://www.sony.net/SonyInfo/News/Press/200710/07-1001E/, accessed: May, **2020**.

[22] a) Samsung Announces GALAXY ROUND in Korea, https://news.samsung.com/global/introducing-galaxy-round-in-korea, accessed: October, **2020**; b) *LG stellt das weltweit erste gebogene Smartphone vor*, https://www.lg.com/at/press-release/images/LG%20G%20Flex%20-%20Erstes%20gebogenes%20Smartphone.pdf, accessed: October, **2020**.

[23] a) R. Mertens, *LG's bendable 77" OLED TV to ship in the second half of 2015*, https://www.oled-info.com/lgs-bendable-77-oled-tv-ship-second-half-2015, accessed: October, **2020**; b) R. Mertens, LG to finally start shipping its 65" rollable OLED TV by the end of October for $100,000, https://www.oled-info.com/lg-finally-start-shipping-its-65-rollable-oled-tv-end-october-100000, accessed: October, **2020**.

[24] a) R. Mertens, *Royole launches a foldable smartphone/tablet developer device*, https://www.oled-info.com/royole-launches-foldable-smartphonetablet-developer-device accessed: October, **2020**; b) *Huawei Launches HUAWEI Mate X,the World's Fastest 5G Foldable Phone*, https://consumer.huawei.com/en/press/news/2019/huawei-launch-mate-x-5g-foldable-phone/, accessed: October, **2020**; c) *Samsung Galaxy Fold Now Available*, https://news.samsung.com/global/samsung-galaxy-fold-now-available accessed: October, **2020**; d) J. Newman, *Introducing the First Foldable Laptop: The Lenovo ThinkPad X1 Fold*, https://www.intel.com/content/www/us/en/products/docs/devices-systems/laptops/laptop-innovation-program/the-first-foldable-laptop.html, accessed: October, **2020**.

[25] N. Rauenbühler, *CYNORA introduces fluorescent blue emitter that gives OLED devices a substantial efficiency boost*, https://cynora.com/cynora-introduces-fluorescent-blue-emitter-that-gives-oled-devices-a-substantial-efficiency-boost/, accessed: October, **2020**.

[26] *Kyulux commences shipment of TADF / Hyperfluorescence™ OLED materials*, https://www.kyulux.com/kyulux-commences-shipment-of-tadf-hyperfluorescence-oled-materials/, accessed: October, **2020**.

[27] a) R. Das, K. Ghaffarzadeh, X. He, Flexible, Printed OLED Displays 2020–2030: *Forecast, Markets, Technologie*, https://www.idtechex.com/de/research-report/flexible-printed-oled-displays-2020-2030-forecasts-markets-technologies/693, accessed: October, **2020**; b) M. Haller, *New CEO and fresh capital for Cynora*, https://www.elektroniknet.de/international/new-ceo-and-fresh-capital-for-cynora-165452.html, accessed: October, **2020**.

[28] *OLED display producers*, https://www.oled-info.com/companies-list/oled-display-producers, accessed: October, **2020**.

[29] a) F. Fell, *cynora: Auf dem Weg zum Weltmarktführer im OLED Bereich*, https://www.techtag.de/digitalisierung/digitale-pioniere/cynora-auf-dem-weg-zum-weltmarktfuehrer-im-oled-bereich-interview/, accessed: October, **2020**; b) C. S. C. Group, CDT – Our History, https://www.cdtltd.co.uk/history/, accessed: October, **2020**; c) D. Microdisplay, https://www.oled-info.com/dresden-microdisplay, accessed: October, **2020**; d) G. Bayes-Brown, *Samsung's lights up spin-outs*, https://globaluniversityventuring.com/samsungs-lights-up-spin-outs/, accessed: October, **2020**; e) *Visionox*, https://www.oled-info.com/visionox, accessed: October, **2020**.

[30] a) *Sumitomo Chemical to Acquire Cambridge Display Technology Inc*, https://www.sumitomo-chem.co.jp/english/news/files/docs/20070731_3.pdf, accessed: October, **2020**; b) *SDI Historical Gallery*, https://www.samsungsdi.com/about-sdi/history.html, accessed: October, **2020**; c) K. Koh, A. Lemke, *Cheil Industries to acquire Novaled AG*, http://www.novaled.com/uploads/media/Press_Release_Cheil_Novaled_acquisition_final.pdf, accessed: October, **2020**.

[31] a) *Kyulux completes its Series B funding round and raises $31.8 million*, https://www.kyulux.com/kyulux-completes-its-series-b-funding-round-and-raises-31-8-million/, accessed: October, **2020**; b) N. Rauenbühler, *OLED materials innovator CYNORA secures US$25M in first closing of Series C Round. CYNORA names Adam Kablanian as new Chief Executive Officer*, https://cynora.com/news-press-release-oled-materials-innovator-cynora-secures-us25m-in-first-closing-of-series-c-round-cynora-names-adam-kablanian-as-new-chief-executive-officer-oled-materials-innovator-cynora-secures-u/, accessed: October, **2020**.

[32] D. S. Jo, M. J. Sung, M. H. Kim, S. C. CHoi, *Journal of KSDT* **2019**, *18*, 105.

[33] C. W. Tang, S. A. VanSlyke, *Appl. Phys. Lett.* **1987**, *51*, 913.

[34] C. W. Tang, S. A. VanSlyke, C. H. Chen, *J. Appl. Phys.* **1989**, *65*, 3610.

[35] C. T. Chen, *Chem. Mater.* **2004**, *16*, 4389.

[36] Y. Hamada, H. Kanno, T. Tsujioka, H. Takahashi, T. Usuki, *Appl. Phys. Lett.* **1999**, *75*, 1682.

[37] S. Toguchi, Y. Morioka, H. Ishikawa, A. Oda, E. Hasegawa, *Synth. Met.* **2000**, *111*, 57.

[38] J. Huang, J.-H. Su, H. Tian, *J. Mater. Chem.* **2012**, *22*, 10977.

[39] C. Adachi, T. Tsutsui, S. Saito, *Appl. Phys. Lett.* **1990**, *56*, 799.

[40] C.-J. Zheng, W.-M. Zhao, Z.-Q. Wang, D. Huang, J. Ye, X.-M. Ou, X.-H. Zhang, C.-S. Lee, S.-T. Lee, *J. Mater. Chem.* **2010**, *20*, 1560.

[41] M. A. Baldo, M. E. Thompson, S. R. Forrest, *Nature* **2000**, *403*, 750.

[42] a) H. Xu, R. Chen, Q. Sun, W. Lai, Q. Su, W. Huang, X. Liu, *Chem. Soc. Rev.* **2014**, *43*, 3259; b) K. Dedeian, P. I. Djurovich, F. O. Garces, G. Carlson, R. J. Watts, *Inorg. Chem.* **1991**, *30*, 1685.

[43] M. A. Baldo, S. Lamansky, P. E. Burrows, M. E. Thompson, S. R. Forrest, *Appl. Phys. Lett.* **1999**, *75*, 4.

[44] A. B. Tamayo, B. D. Alleyne, P. I. Djurovich, S. Lamansky, I. Tsyba, N. N. Ho, R. Bau, M. E. Thompson, *J. Am. Chem. Soc.* **2003**, *125*, 7377.

[45] W. C. Choy, W. K. Chan, Y. Yuan, *Adv. Mater.* **2014**, *26*, 5368.

[46] S. Lamansky, P. Djurovich, D. Murphy, F. Abdel-Razzaq, H. E. Lee, C. Adachi, P. E. Burrows, S. R. Forrest, M. E. Thompson, *J. Am. Chem. Soc.* **2001**, *123*, 4304.

[47] G. Zhou, C.-L. Ho, W.-Y. Wong, Q. Wang, D. Ma, L. Wang, Z. Lin, T. B. Marder, A. Beeby, *Adv. Funct. Mater.* **2008**, *18*, 499.

[48] a) J. Li, P. I. Djurovich, B. D. Alleyne, M. Yousufuddin, N. N. Ho, J. C. Thomas, J. C. Peters, R. Bau, M. E. Thompson, *Inorg. Chem.* **2005**, *44*, 1713; b) H. J. Bolink, F. De Angelis, E. Baranoff, C. Klein, S. Fantacci, E. Coronado, M. Sessolo, K. Kalyanasundaram, M. Gratzel, M. K. Nazeeruddin, *Chem. Commun.* **2009**, 4672; c) Y. Kawamura, K. Goushi, J. Brooks, J. J. Brown, H. Sasabe, C. Adachi, *Appl. Phys. Lett.* **2005**, *86*, 071104.

[49] J. Ding, J. Gao, Y. Cheng, Z. Xie, L. Wang, D. Ma, X. Jing, F. Wang, *Adv. Funct. Mater.* **2006**, *16*, 575.

[50] K.-H. Kim, C.-K. Moon, J.-H. Lee, S.-Y. Kim, J.-J. Kim, *Adv. Mater.* **2014**, *26*, 3844.

[51] a) B. D'Andrade, S. R. Forrest, *Chem. Phys.* **2003**, *286*, 321; b) B. W. D'Andrade, J. Brooks, V. Adamovich, M. E. Thompson, S. R. Forrest, *Adv. Mater.* **2002**, *14*, 1032. c) V. Adamovich, J. Brooks, A. Tamayo, A. M. Alexander, P. I. Djurovich, B. W. D'Andrade, C. Adachi, S. R. Forrest, M. E. Thompson, *New J. Chem.* **2002**, *26*, 1171.

[52] a) W. Lu, M. C. W. Chan, K.-K. Cheung, C.-M. Che, *Organometallics* **2001**, *20*, 2477; b) S. J. Farley, D. L. Rochester, A. L. Thompson, J. A. Howard, J. A. Williams, *Inorg. Chem.* **2005**, *44*, 9690.

[53] M. Cocchi, D. Virgili, V. Fattori, D. L. Rochester, J. A. G. Williams, *Adv. Funct. Mater.* **2007**, *17*, 285.

**ADVANCED
SCIENCE NEWS**

www.advancedsciencenews.com

**ADVANCED
MATERIALS**

www.advmat.de

[54] P. K. Chow, G. Cheng, G. S. Tong, W. P. To, W. L. Kwong, K. H. Low, C. C. Kwok, C. Ma, C. M. Che, *Angew. Chem., Int. Ed. Engl.* **2015**, *54*, 2084.

[55] V. K. Au, K. M. Wong, D. P. Tsang, M. Y. Chan, N. Zhu, V. W. Yam, *J. Am. Chem. Soc.* **2010**, *132*, 14273.

[56] a) M. C. Tang, C. H. Lee, M. Ng, Y. C. Wong, M. Y. Chan, V. W. Yam, *Angew. Chem., Int. Ed. Engl.* **2018**, *57*, 5463; b) M. C. Tang, D. P. Tsang, M. M. Chan, K. M. Wong, V. W. Yam, *Angew. Chem., Int. Ed. Engl.* **2013**, *52*, 446; c) M. C. Tang, C. H. Lee, S. L. Lai, M. Ng, M. Y. Chan, V. W. Yam, *J. Am. Chem. Soc.* **2017**, *139*, 9341; d) C. H. Lee, M. C. Tang, W. L. Cheung, S. L. Lai, M. Y. Chan, V. W. Yam, *Chem. Sci.* **2018**, *9*, 6228; e) H. Beucher, S. Kumar, E. Merino, W.-H. Hu, G. Stemmler, S. Cuesta-Galisteo, J. A. González, J. Jagielski, C.-J. Shih, C. Nevado, *Chem. Mater.* **2020**, *32*, 1605.

[57] M. Hashimoto, S. Igawa, M. Yashima, I. Kawata, M. Hoshino, M. Osawa, *J. Am. Chem. Soc.* **2011**, *133*, 10348.

[58] M. A. Baldo, D. F. O'Brien, Y. You, A. Shoustikov, S. Sibley, M. E. Thompson, S. R. Forrest, *Nature* **1998**, *395*, 151.

[59] C. Zhang, R. H. Liu, D. D. Zhang, L. Duan, *Adv. Funct. Mater.* **2020**, *30*, 1907156.

[60] H. Xiang, J. Cheng, X. Ma, X. Zhou, J. J. Chruma, *Chem. Soc. Rev.* **2013**, *42*, 6128.

[61] A. Tsuboyama, H. Iwawaki, M. Furugori, T. Mukaide, J. Kamatani, S. Igawa, T. Moriyama, S. Miura, T. Takiguchi, S. Okada, M. Hoshino, K. Ueno, *J. Am. Chem. Soc.* **2003**, *125*, 12971.

[62] G. Zhou, W. Y. Wong, B. Yao, Z. Xie, L. Wang, *Angew. Chem., Int. Ed. Engl.* **2007**, *46*, 1149.

[63] D. H. Kim, N. S. Cho, H. Y. Oh, J. H. Yang, W. S. Jeon, J. S. Park, M. C. Suh, J. H. Kwon, *Adv. Mater.* **2011**, *23*, 2721.

[64] X. Yang, H. Guo, B. Liu, J. Zhao, G. Zhou, Z. Wu, W. Y. Wong, *Adv. Sci.* **2018**, *5*, 1800950.

[65] M. Cocchi, J. Kalinowski, D. Virgili, J. A. G. Williams, *Appl. Phys. Lett.* **2008**, *92*, 113302.

[66] T. Fleetham, G. Li, J. Li, *ACS Appl. Mater. Interfaces* **2015**, *7*, 16240.

[67] K. Tuong Ly, R.-W. Chen-Cheng, H.-W. Lin, Y.-J. Shiau, S.-H. Liu, P.-T. Chou, C.-S. Tsao, Y.-C. Huang, Y. Chi, *Nat. Photonics* **2016**, *11*, 63.

[68] C. Adachi, M. A. Baldo, S. R. Forrest, S. Lamansky, M. E. Thompson, R. C. Kwong, *Appl. Phys. Lett.* **2001**, *78*, 1622.

[69] a) S.-J. Su, C. Cai, J. Kido, *J. Mater. Chem.* **2012**, *22*, 3447; b) X. Ren, J. Li, R. J. Holmes, P. I. Djurovich, S. R. Forrest, M. E. Thompson, *Chem. Mater.* **2004**, *16*, 4743.

[70] X. Yang, X. Xu, G. Zhou, *J. Mater. Chem. C* **2015**, *3*, 913.

[71] K. S. Yook, J. Y. Lee, *Org. Electron.* **2011**, *12*, 1711.

[72] J. Lee, H. F. Chen, T. Batagoda, C. Coburn, P. I. Djurovich, M. E. Thompson, S. R. Forrest, *Nat. Mater.* **2016**, *15*, 92.

[73] B. Ma, P. I. Djurovich, S. Garon, B. Alleyne, M. E. Thompson, *Adv. Funct. Mater.* **2006**, *16*, 2438.

[74] a) T. Fleetham, G. Li, L. Wen, J. Li, *Adv. Mater.* **2014**, *26*, 7116; b) X.-C. Hang, T. Fleetham, E. Turner, J. Brooks, J. Li, *Angew. Chem.* **2013**, *125*, 6885.

[75] H. Shin, Y. H. Ha, H. G. Kim, R. Kim, S. K. Kwon, Y. H. Kim, J. J. Kim, *Adv. Mater.* **2019**, *31*, 1808102.

[76] Z. Yang, Z. Mao, Z. Xie, Y. Zhang, S. Liu, J. Zhao, J. Xu, Z. Chi, M. P. Aldred, *Chem. Soc. Rev.* **2017**, *46*, 915.

[77] A. Endo, K. Sato, K. Yoshimura, T. Kai, A. Kawada, H. Miyazaki, C. Adachi, *Appl. Phys. Lett.* **2011**, *98*, 083302.

[78] H. Uoyama, K. Goushi, K. Shizu, H. Nomura, C. Adachi, *Nature* **2012**, *492*, 234.

[79] P. Rajamalli, N. Senthilkumar, P. Gandeepan, P. Y. Huang, M. J. Huang, C. Z. Ren-Wu, C. Y. Yang, M. J. Chiu, L. K. Chu, H. W. Lin, C. H. Cheng, *J. Am. Chem. Soc.* **2016**, *138*, 628.

[80] M. Li, Y. Liu, R. Duan, X. Wei, Y. Yi, Y. Wang, C. F. Chen, *Angew. Chem., Int. Ed. Engl.* **2017**, *56*, 8818.

[81] D. Zhang, X. Song, M. Cai, H. Kaji, L. Duan, *Adv. Mater.* **2018**, *30*, 1705406.

[82] T. L. Wu, M. J. Huang, C. C. Lin, P. Y. Huang, T. Y. Chou, R. W. Chen-Cheng, H. W. Lin, R. S. Liu, C. H. Cheng, *Nat. Photonics* **2018**, *12*, 235.

[83] a) T. Hatakeyama, K. Shiren, K. Nakajima, S. Nomura, S. Nakatsuka, K. Kinoshita, J. Ni, Y. Ono, T. Ikuta, *Adv. Mater.* **2016**, *28*, 2777; b) Y. Zhang, D. Zhang, J. Wei, Z. Liu, Y. Lu, L. Duan, *Angew. Chem.* **2019**, *131*, 17068.

[84] Y. Yuan, X. Tang, X. Y. Du, Y. Hu, Y. J. Yu, Z. Q. Jiang, L. S. Liao, S. T. Lee, *Adv. Opt. Mater.* **2019**, *7*, 1801536.

[85] N. Ikeda, S. Oda, R. Matsumoto, M. Yoshioka, D. Fukushima, K. Yoshiura, N. Yasuda, T. Hatakeyama, *Adv. Mater.* **2020**, *32*, 2004072.

[86] J. C. Deaton, S. C. Switalski, D. Y. Kondakov, R. H. Young, T. D. Pawlik, D. J. Giesen, S. B. Harkins, A. J. Miller, S. F. Mickenberg, J. C. Peters, *J. Am. Chem. Soc.* **2010**, *132*, 9499.

[87] D. Volz, D. M. Zink, T. Bocksrocker, J. Friedrichs, M. Nieger, T. Baumann, U. Lemmer, S. Bräse, *Chem. Mater.* **2013**, *25*, 3414.

[88] D. Volz, Y. Chen, M. Wallesch, R. Liu, C. Flechon, D. M. Zink, J. Friedrichs, H. Flugge, R. Steininger, J. Gottlicher, C. Heske, L. Weinhardt, S. Bräse, F. So, T. Baumann, *Adv. Mater.* **2015**, *27*, 2538.

[89] a) A. Verma, D. M. Zink, C. Flechon, J. L. Carballo, H. Flugge, J. M. Navarro, T. Baumann, D. Volz, *Appl. Phys. A* **2016**, *122*, 191. b) M. Wallesch, A. Verma, C. Flechon, H. Flugge, D. M. Zink, S. M. Seifermann, J. M. Navarro, T. Vitova, J. Gottlicher, R. Steininger, L. Weinhardt, M. Zimmer, M. Gerhards, C. Heske, S. Bräse, T. Baumann, D. Volz, *Chemistry* **2016**, *22*, 16400; c) J. M. Busch, D. M. Zink, P. Di Martino-Fumo, F. R. Rehak, P. Boden, S. Steiger, O. Fuhr, M. Nieger, W. Klopper, M. Gerhards, S. Bräse, *Dalton Trans.* **2019**, *48*, 15687.

[90] X.-L. Chen, C.-S. Lin, X.-Y. Wu, R. Yu, T. Teng, Q.-K. Zhang, Q. Zhang, W.-B. Yang, C.-Z. Lu, *J. Mater. Chem. C* **2015**, *3*, 1187.

[91] G. U. Mahoro, J. Fernandez-Cestau, J. L. Renaud, P. B. Coto, R. D. Costa, S. Gaillard, *Adv. Opt. Mater.* **2020**, *8*, 2000260.

[92] W. P. To, D. Zhou, G. S. M. Tong, G. Cheng, C. Yang, C. M. Che, *Angew. Chem., Int. Ed.* **2017**, *56*, 14036.

[93] A. S. Romanov, D. Di, L. Yang, J. Fernandez-Cestau, C. R. Becker, C. E. James, B. Zhu, M. Linnolahti, D. Credgington, M. Bochmann, *Chem. Commun.* **2016**, *52*, 6379.

[94] a) M. Gernert, U. Muller, M. Haehnel, J. Pflaum, A. Steffen, *Chemistry* **2017**, *23*, 2206; b) A. S. Romanov, C. R. Becker, C. E. James, D. Di, D. Credgington, M. Linnolahti, M. Bochmann, *Chemistry* **2017**, *23*, 4625; c) A. S. Romanov, F. Chotard, J. Rashid, M. Bochmann, *Dalton Trans.* **2019**, *48*, 15445.

[95] S. Shi, M. C. Jung, C. Coburn, A. Tadle, M. R. D. Sylvinson, P. I. Djurovich, S. R. Forrest, M. E. Thompson, *J. Am. Chem. Soc.* **2019**, *141*, 3576.

[96] a) A. S. Romanov, S. T. E. Jones, Q. Gu, P. J. Conaghan, B. H. Drummond, J. Feng, F. Chotard, L. Buizza, M. Foley, M. Linnolahti, D. Credgington, M. Bochmann, *Chem. Sci.* **2020**, *11*, 435; b) B. Rao, H. Tang, X. Zeng, L. Liu, M. Melaimi, G. Bertrand, *Angew. Chem., Int. Ed. Engl.* **2015**, *54*, 14915; c) T. Y. Li, D. S. Muthiah Ravinson, R. Haiges, P. I. Djurovich, M. E. Thompson, *J. Am. Chem. Soc.* **2020**, *142*, 6158; d) R. Hamze, S. Shi, S. C. Kapper, D. S. Muthiah Ravinson, L. Estergreen, M. C. Jung, A. C. Tadle, R. Haiges, P. I. Djurovich, J. L. Peltier, R. Jazzar, G. Bertrand, S. E. Bradforth, M. E. Thompson, *J. Am. Chem. Soc.* **2019**, *141*, 8616.

[97] J. Li, T. Nakagawa, J. MacDonald, Q. Zhang, H. Nomura, H. Miyazaki, C. Adachi, *Adv. Mater.* **2013**, *25*, 3319.

[98] P. Data, P. Pander, M. Okazaki, Y. Takeda, S. Minakata, A. P. Monkman, *Angew. Chem.* **2016**, *128*, 5833.

[99] W. Zeng, H. Y. Lai, W. K. Lee, M. Jiao, Y. J. Shiu, C. Zhong, S. Gong, T. Zhou, G. Xie, M. Sarma, K. T. Wong, C. C. Wu, C. Yang, *Adv. Mater.* **2018**, *30*, 1704961.

[100] C. M. Hsieh, T. L. Wu, J. Jayakumar, Y. C. Wang, C. L. Ko, W. Y. Hung, T. C. Lin, H. H. Wu, K. H. Lin, C. H. Lin, S. Hsieh, C. H. Cheng, *ACS Appl. Mater. Interfaces* **2020**, *12*, 23199.

[101] S. Wang, X. Yan, Z. Cheng, H. Zhang, Y. Liu, Y. Wang, *Angew. Chem., Int. Ed. Engl.* **2015**, *54*, 13068.

[102] W. Zeng, T. Zhou, W. Ning, C. Zhong, J. He, S. Gong, G. Xie, C. Yang, *Adv. Mater.* **2019**, *31*, 1901404.

[103] Y. L. Zhang, Q. Ran, Q. Wang, Y. Liu, C. Hanisch, S. Reineke, J. Fan, L. S. Liao, *Adv. Mater.* **2019**, *31*, 1902368.

[104] a) J. H. Kim, J. H. Yun, J. Y. Lee, *Adv. Opt. Mater.* **2018**, *6*, 1800255; b) Y. Zhang, Y. Wang, J. Song, J. Qu, B. Li, W. Zhu, W.-Y. Wong, *Adv. Opt. Mater.* **2018**, *6*, 1800466.

[105] a) V. A. Krylova, P. I. Djurovich, M. T. Whited, M. E. Thompson, *Chem. Commun.* **2010**, *46*, 6696; b) B. Hupp, C. Schiller, C. Lenczyk, M. Stanoppi, K. Edkins, A. Lorbach, A. Steffen, *lnorg. Chem.* **2017**, *56*, 8996.

[106] G. K. So, G. Cheng, J. Wang, X. Chang, C. C. Kwok, H. Zhang, C. M. Che, *Chem.— Asian J.* **2017**, *12*, 1490.

[107] J.-H. Lee, C.-H. Chen, P.-H. Lee, H.-Y. Lin, M.-K. Leung, T.-L. Chiu, C.-F. Lin, *J. Mater. Chem. C* **2019**, *7*, 5874.

[108] C. Murawski, K. Leo, M. C. Gather, *Adv. Mater.* **2013**, *25*, 6801.

[109] Q. Zhang, J. Li, K. Shizu, S. Huang, S. Hirata, H. Miyazaki, C. Adachi, *J. Am. Chem. Soc.* **2012**, *134*, 14706.

[110] Q. Zhang, B. Li, S. Huang, H. Nomura, H. Tanaka, C. Adachi, *Nat. Photonics* **2014**, *8*, 326.

[111] W. L. Tsai, M. H. Huang, W. K. Lee, Y. J. Hsu, K. C. Pan, Y. H. Huang, H. C. Ting, M. Sarma, Y. Y. Ho, H. C. Hu, C. C. Chen, M. T. Lee, K. T. Wong, C. C. Wu, *Chem. Commun.* **2015**, *51*, 13662.

[112] T. A. Lin, T. Chatterjee, W. L. Tsai, W. K. Lee, M. J. Wu, M. Jiao, K. C. Pan, C. L. Yi, C. L. Chung, K. T. Wong, C. C. Wu, *Adv. Mater.* **2016**, *28*, 6976.

[113] C. Y. Chan, L. S. Cui, J. U. Kim, H. Nakanotani, C. Adachi, *Adv. Funct. Mater.* **2018**, *28*, 1706023.

[114] J. Jayakumar, T. L. Wu, M. J. Huang, P. Y. Huang, T. Y. Chou, H. W. Lin, C. H. Cheng, *ACS Appl. Mater. Interfaces* **2019**, *11*, 21042.

[115] T. Ohsawa, H. Sasabe, T. Watanabe, K. Nakao, R. Komatsu, Y. Hayashi, Y. Hayasaka, J. Kido, *Adv. Opt. Mater.* **2019**, *7*, 1801282.

[116] X. Zeng, K.-P. Pan, W.-K. Lee, S. Gong, F. Ni, X. Xiao, W. Zeng, Y. Xiang, L. Zhan, Y. Zhang, C.-C. Wu, C. Yang, *J. Mater. Chem. C* **2019**, *7*, 10851.

[117] D. Hall, S. M. Suresh, P. L. dos Santos, E. Duda, S. Bagnich, A. Pershin, P. Rajamalli, D. B. Cordes, A. M. Z. Slawin, D. Beljonne, A. Köhler, I. D. W. Samuel, Y. Olivier, E. Zysman-Colman, *Adv. Opt. Mater.* **2020**, *8*, 1901627.

[118] Z. Zhang, E. Crovini, P. L. dos Santos, B. A. Naqvi, D. B. Cordes, A. M. Z. Slawin, P. Sahay, W. Brütting, I. D. W. Samuel, S. Bräse, E. Zysman-Colman, *Adv. Opt. Mater.* **2020**, 2001354.

[119] F.-M. Xie, Z.-D. An, M. Xie, Y.-Q. Li, G.-H. Zhang, S.-J. Zou, L. Chen, J.-D. Chen, T. Cheng, J.-X. Tang, *J. Mater. Chem. C* **2020**, *8*, 5769.

[120] V. V. Patil, K. H. Lee, J. Y. Lee, *Dyes Pigm.* **2020**, *174*, 108070.

[121] R. Hamze, J. L. Peltier, D. Sylvinson, M. Jung, J. Cardenas, R. Haiges, M. Soleilhavoup, R. Jazzar, P. I. Djurovich, G. Bertrand, M. E. Thompson, *Science* **2019**, *363*, 601.

[122] a) C. Eickhoff, P. Murer, T. Geßner, J. Birnstock, M. Kröger, Z. Choi, S. Watanabe, F. May, C. Lennartz, I. Stengel, I. Münster, K. Kahle, G. Wagenblast, H. Mangold, *SPIE Organic Photonics + Electronics*, SPIE, San Diego **2015**; b) J. Hu, S. Hu, C. Lu, Y. Huang, K. Xu, X. Wang, *J. Lumin.* **2018**, *197*, 187; c) D. Sun, Z. Ren, S. Yan, *J. Mater. Chem. C* **2018**, *6*, 4800.

[123] J. Adachi, H. Kakizoe, P. K. D. Tsang, A. Endo, *Dig. Tech. Pap.— Soc. Inf. Disp. Int. Symp.* **2019**, *50*, 95.

[124] a) C. Adachi, *Dig. Tech. Pap.— Soc. Inf. Disp. Int. Symp.* **2013**, *44*, 513; b) A. M. Polgar, C. M. Tonge, C. J. Christopherson, N. R. Paisley, A. C. Reyes, Z. M. Hudson, *ACS Appl. Mater. Interfaces* **2020**, *12*, 38602.

[125] H. Nakanotani, T. Higuchi, T. Furukawa, K. Masui, K. Morimoto, M. Numata, H. Tanaka, Y. Sagara, T. Yasuda, C. Adachi, *Nat. Commun.* **2014**, *5*, 4016.

[126] S. H. Han, J. Y. Lee, *J. Mater. Chem. C* **2018**, *6*, 1504.

[127] S. K. Jeon, H. J. Park, J. Y. Lee, *ACS Appl. Mater. Interfaces* **2018**, *10*, 5700.

[128] J. S. Jang, S. H. Han, H. W. Choi, K. S. Yook, J. Y. Lee, *Org. Electron.* **2018**, *59*, 236.

[129] a) T. Baumann, M. Budzynski, C. Kasparek, *Dig. Tech. Pap.— Soc. Inf. Disp. Int. Symp.* **2019**, *50*, 466; b) D. Thirion, C. Kasparek, T. Baumann, *Dig. Tech. Pap.— Soc. Inf. Disp. Int. Symp.* **2019**, *50*, 497.

[130] S. Gottardi, M. Barbry, R. Coehoorn, H. Van Eersel, *Appl. Phys. Lett.* **2019**, *114*, 073301.

[131] M. Jakoby, B. S. Richards, U. Lemmer, I. A. Howard, *Phys. Rev. B* **2019**, *100*, 045303.

[132] J. H. Kim, K. H. Lee, J. Y. Lee, *J. Mater. Chem. C* **2020**, *8*, 5265.

[133] J. H. Yun, K. H. Lee, J. Y. Lee, *Dyes Pigm.* **2020**, *181*, 108549.

[134] K. H. Kim, C. K. Moon, J. W. Sun, B. Sim, J. J. Kim, *Adv. Opt. Mater.* **2015**, *3*, 895.

[135] D. Li, Y. Hu, L.-S. Liao, *J. Mater. Chem. C* **2019**, *7*, 977.

[136] K. H. Lee, J. Y. Lee, *Adv. Opt. Mater.* **2020**, *8*, 2000328.

[137] J. Yao, Z. Wang, X. Qiao, D. Yang, Y. Dai, Q. Sun, J. Chen, C. Yang, D. Ma, *Org. Electron.* **2020**, *84*, 105824.

[138] a) H. Yersin, L. Mataranga-Popa, S.-W. Li, R. Czerwieniec, *Dig. Tech. Pap.— Soc. Inf. Disp. Int. Symp.* **2018**, *49*, 48; b) H. Yersin, L. Mataranga-Popa, R. Czerwieniec, Y. Dovbii, *Chem. Mater.* **2019**, *31*, 6110.

[139] R. Haldar, L. Heinke, C. Woll, *Adv. Mater.* **2020**, *32*, 1905227.

[140] H. Mieno, R. Kabe, M. D. Allendorf, C. Adachi, *Chem. Commun.* **2018**, *54*, 631.

[141] C. Woll, R. Haldar, M. Jakoby, M. Kozlowska, M. R. Khan, H. Chen, Y. Pramudya, B. S. Richards, L. Heinke, W. Wenzel, F. Odobel, S. Diring, I. A. Howard, U. Lemmer, *Chem. Eur. J.* **2020**, *26*, 1.

[142] D.-W. Zhang, M. Li, C.-F. Chen, *Chem. Soc. Rev.* **2020**, *49*, 1331.

[143] J. R. Brandt, X. Wang, Y. Yang, A. J. Campbell, M. J. Fuchter, *J. Am. Chem. Soc.* **2016**, *138*, 9743.

[144] N. Sharma, E. Spuling, C. M. Mattern, W. Li, O. Fuhr, Y. Tsuchiya, C. Adachi, S. Bräse, I. D. W. Samuel, E. Zysman-Colman, *Chem. Sci.* **2019**, *10*, 6689.

**ADVANCED
SCIENCE NEWS**

www.advancedsciencenews.com

**ADVANCED
MATERIALS**

www.advmat.de

Gloria Hong obtained her B.Sc. (2016) and M.Sc. degrees (2019) in Chemistry from TU Munich (Germany). During her studies she spent a semester at the Technion Israel Institute of Technology (Israel) and did her master thesis project at TU Berlin (Germany). She joined the Bräse group at KIT (Germany) in 2019 as a Ph.D. student and is currently obtaining an MBA from the Collège des Ingénieurs (CDI) in parallel. As a member of the research training group RTG 2039, her research is focused on the synthesis of red TADF emitters for OLED and imaging applications.

Xuemin Gan received her B.Sc. degree (2015) in Applied Chemistry from Chongqing University (CQU, China) and her M.Sc. degree (2018) in Physical Chemistry from the Fujian Institute of Research on the Structure of Matter, Chinese Academy of Sciences (FJIRSM-CAS), under the supervision of Prof. Can-Zhong Lu. Currently, she is a Ph.D. student at the KIT under the mentorship of Prof. S. Bräse. Her research interests are the synthesis of luminescent Cu(I) complexes and their application in OLEDs.

Céline Leonhardt obtained her B.Sc. (2018) and her M.Sc. (2020) degree in Chemistry from the KIT. During her Master's studies (2018–2019) she stayed for a research project in the research group of Prof. G. Deacon working on C—F activation with rare-earth elements for three months at the Monash University in Melbourne (Australia). In 2020, she began her doctoral research in advanced TADF emitters for OLED applications at the KIT in the research group of Prof. S. Bräse.
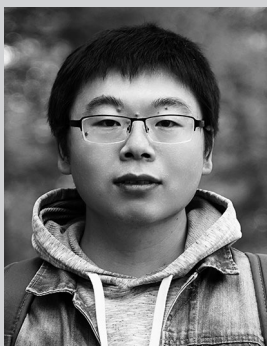
Zhen Zhang obtained his M.Sc. degree (2016) in Chemistry from Shanghai University (China). He then began his doctoral research at the Institute of Organic Chemistry (IOC), KIT under the mentorship of Prof. S. Bräse. He received his Ph.D. in 2020 for his work on the design and synthesis of *N*-heterocyclic donor-based TADF emitters for application in OLEDs. Zhen Zhang is currently a PostDoc in the Bräse group and his research focuses on the design and synthesis of novel organic luminophors for optoelectronic devices.

Jasmin Seibert received her B.Sc. degree in Chemistry from the KIT in 2018. After a research stay in the research group of Prof. L. L. Schafer working on early transition metal-catalyzed hydroaminoalkylation at the University of British Columbia in Vancouver (Canada), she completed her M.Sc. degree in 2020. Currently, she is a Ph.D. candidate in the group of Prof. S. Bräse, working on optoelectronic materials based on the [2.2]paracyclophane framework.

Jasmin M. Busch obtained her B.Sc. (2014) and M.Sc. degree (2017) in Chemistry from the Goethe University (Frankfurt, Germany). In 2017, she began her doctoral research at the KIT (Prof. S. Bräse) and was a fellow of the Karlsruhe School of Optics and Photonics (KSOP). After a research stay in 2019 at the University of St. Andrews (Prof. E. Zysman-Colman), she received her Ph.D. in 2020 for her work on the synthesis of Cu(I) and Ag(I) complexes for the investigation of cooperative effects and application in OLEDs. Jasmin M. Busch is currently a PostDoc in the Bräse group.

Stefan Bräse studied in Göttingen (Germany), Bangor (UK.) and Marseille (France) and received his Ph.D. in 1995 (Armin de Meijere, Göttingen). After postdoctoral research at Uppsala University (Jan E. Bäckvall) and Scripps Research Institute (K. C. Nicolaou), he began his independent research career at RWTH Aachen (1997, Dieter Enders). In 2001, he finished his habilitation and became professor for Organic Chemistry at the University of Bonn. Since 2003, he is professor at the Institute of Organic Chemistry, KIT and since 2012, also the director of the Institute of Biological and Chemical Systems (IBCS) (formerly Toxicology and Genetics (ITG)) at KIT.